Chemical Geology
November 2013, Volume 359, Pages 136-149
http://dx.doi.org/10.1016/j.chemgeo.2013.10.001

Native Cu from the oceanic crust: Isotopic insights into native metal origin

Vesselin M. Dekov[a, *], Olivier Rouxel[a, b], Dan Asael[a], Ulf Hålenius[c], Frans Munnik[d]

[a] IFREMER, Centre de Brest, Department of Marine Geosciences, 29280 Plouzané, France
[b] Marine Chemistry and Geochemistry Department, Woods Hole Oceanographic Institution, Woods Hole, MA 02543, USA
[c] Department of Mineralogy, Swedish Museum of Natural History, Box 50007, SE-104 05 Stockholm, Sweden
[d] Institute of Ion Beam Physics and Materials Research, Helmholtz-Zentrum Dresden-Rossendorf, D-01328 Dresden, Germany

*: Corresponding author : Vesselin M. Dekov, tel.: + 33 2 98 22 49 53 ; fax: + 33 2 98 22 45 70 ;
email address : Vesselin.Dekov@ifremer.fr

Abstract:

Ocean drilling has revealed that, although a minor mineral phase, native Cu ubiquitously occurs in the oceanic crust. Cu isotope systematics for native Cu from a set of occurrences from volcanic basement and sediment cover of the oceanic crust drilled at several sites in the Pacific, Atlantic and Indian oceans constrains the sources of Cu and processes that produced Cu^0. We propose that both hydrothermally-released Cu and seawater were the sources of Cu at these sites. Phase stability diagrams suggest that Cu^0 precipitation is favored only under strictly anoxic, but not sulfidic conditions at circum-neutral pH even at low temperature. In the basaltic basement, dissolution of primary igneous and potentially hydrothermal Cu-sulfides leads to Cu^0 precipitation along veins. The restricted Cu-isotope variations ($\delta^{65}Cu$ = 0.02 – 0.19‰) similar to host volcanic rocks suggest that Cu^0 precipitation occurred under conditions where Cu^+-species were dominant, precluding Cu redox fractionation. In contrast, the Cu-isotope variations observed in the Cu^0 from sedimentary layers yield larger Cu-isotope fractionation ($\delta^{65}Cu$ = 0.41 – 0.95‰) suggesting that Cu^0 precipitation involved redox processes during the diagenesis, with potentially seawater as the primary Cu source. We interpret that native Cu precipitation in the basaltic basement is a result of low temperature (20°-65 °C) hydrothermal processes under anoxic, but not H_2S-rich conditions. Consistent with positive $\delta^{65}Cu$ signatures, the sediment cover receives major Cu contribution from hydrogenous (i.e., seawater) sources, although hydrothermal contribution from plume fallout cannot be entirely discarded. In this case, disseminated hydrogenous and/or hydrothermal Cu might be diagenetically remobilized and reprecipitated as Cu^0 in reducing microenvironment.

Highlights

► native Cu is a minor mineral phase in the oceanic crust ► Cu^0 precipitation is favored under anoxic, but not sulfidic conditions at pH ~ 7 ► Cu^+-species are dominant in the basaltic basement ► Cu^{2+}-species dominate in the solutions in the sedimentary layer ► Cu^0 precipitation in the basaltic basement is related to seawater-rock interaction ► sediment cover receives major Cu contribution from hydrogenous (seawater) source.

Keywords : Cu-isotopes ; Deep-Sea Drilling Project ; native Cu ; Ocean Drilling Project ; oceanic crust alteration

1. Introduction

Copper is amongst the elements which most commonly occur in zero-valence state in nature. As such, native Cu (Cu^0) deposits have long been one of the most important Cu resources

(e.g., Wang et al., 2006; Cooper et al., 2008; Pinto et al., 2011). In general, the large Cu^0 deposits are genetically related to either magmatic or hydrothermal Cu-sulfide deposits (Cornwall, 1956; Amstutz, 1977; Brown, 2006) and are often considered to form as products of their supergene alteration. Although our knowledge on Cu^0 mode of formation is based almost exclusively on occurrences from the continents where it occurs in a wide range of rocks, Cu^0 has been reported to occur in fragments of ancient oceanic crust (ophiolites) (Nagle et al., 1973; Abrajano and Pasteris, 1989; Bai et al., 2000; Miller et al., 2003; Ikehata et al., 2011), in the igneous basement of the recent oceanic crust (von der Borch et al., 1974; Kennett et al., 1975; Ovenshine et al., 1975; Talwani et al., 1976; Roberts et al., 1984; Leinen et al., 1986; LeHuray, 1989; Puchelt et al., 1996), in marine sediments (Berger and von Rad, 1972; Hollister et al., 1972; Zemmels et al., 1972; Schlanger et al., 1976; Siesser, 1978; Knox, 1985; Jenkyns, 1976; Marchig et al., 1986; Dekov et al., 1999) and in seafloor massive sulfides (Minniti and Bonavia, 1984; Hannington et al., 1988). Almost all these works but two (Hannington et al., 1988; Dekov et al., 1999) are either brief reports of Cu^0 occurrences without any particular study of the mineral, or mere speculations on the native Cu origin. There is no systematic study on Cu^0 from the oceanic crust and, therefore, we know little about the Cu^0 formation in this setting.

Recent development in mass spectrometry techniques has led to a tremendous growth of research on transitional metal isotopes such as Fe, Cu, Zn and Mo (Johnson et al., 2004; Anbar and Rouxel, 2007). In their pioneering work on the natural variations of the Cu-isotopes ^{65}Cu and ^{63}Cu, Walker et al. (1958) and Shields et al. (1965) reported Cu-isotope variations of several per mil in Cu-ores. These results were confirmed by later more precise isotope measurements using multicollector inductively-coupled plasma mass-spectrometry (MC-ICP-MS) (Maréchal et al., 1999; Zhu et al., 2000; Larson et al., 2003; Graham et al., 2004; Rouxel et al., 2004; Mason et al., 2005; Maher and Larson, 2007; Mathur et al., 2009; Palacios et al., 2011). This new capability

for Cu-isotope measurement demonstrates the great potential of Cu-isotopes as new tracers for the study of modern and ancient hydrothermal systems and Cu deposits [skarn (Maher and Larson, 2007), porphyry (Mathur et al., 2009) and supergene (Mathur et al., 2005)]. In particular, it is hoped that Cu-isotopes may provide a powerful tool for getting insights into the source of Cu and the mechanisms of Cu^0 mineralization in the oceanic crust.

In this study we have investigated a set of native Cu occurrences from a range of basement rocks and sediments drilled at several Deep-Sea Drilling Project (DSDP) and Ocean Drilling Project (ODP) sites aiming at: (1) characterization of Cu^0 from the oceanic crust; (2) determining the sources of Cu and the processes that produced Cu^0 with an ultimate goal to set a ground for further interpretations of the origin of native Cu deposits on land.

2. Geologic setting

We present brief lithologic-stratigraphic descriptions of the DSDP/ODP cores (from top to bottom) where we have found Cu^0 particles, with more particular attention to the core units with native Cu findings. Details on lithology and stratigraphy of the investigated cores can be found elsewhere (Hollister et al., 1972; von der Borch et al., 1974; Bolli et al., 1978; Leinen et al., 1986; Eldholm et al., 1987).

2.1. Site 105

The cored section at Site 105 (DSDP Leg 11) starts with silty hemipelagic clay (Q) overlying hemipelagic clay (Tertiary), multicolored clay [K_2^{cm}(?) – Pg_2(?)], black clay (K_1^{bar} – K_2^{cm}), white and gray limestone (J_3^{tit} – Neocomian), red clayey limestone ($J_3^{ox\text{-}kim}$) and basalt (J_3)

(Fig. 1; Hollister et al., 1972). A vein of tiny Cu^0 crystals occurs in the pale red, reddish-brown and greenish intercalations of clayey limestone ~10 m above the basalt unit (Fig. 1). This limestone is composed of calcite, clays, hematite and quartz and shows a variety of slump structures. The Cu^0 vein is bordered by palagonite and it also shows palagonite filling the interstices between Cu^0 crystals. The clayey limestone covers pyroclastics that are altered to montmorillonite. Below the pyroclastics recrystallized limestones (with high-Mg calcite) occur at the contact with the underlying basalt that is highly fractured (veins of calcite) and altered.

2.2. Site 216

Drilling at Site 216 (DSDP Leg 22) cored sediments composed of nannofossil ooze and chalk with foraminifera ($Pg_3^3 - Q_1$), nannofossil chalk ($Pg_1 - Pg_3^3$), glauconite-bearing micarb chalk and ash-bearing volcanic clay (K_2^{ms}), and basalt (Fig. 1; von der Borch et al., 1974). The recovered basement section is divided into four units (from top to bottom): (1) sediment-basement interface consisting of a chlorite-rich limestone mixed with volcanic debris; (2) thin flows (< l m thick) of medium dark gray vesicular and amygdaloidal basalts intercalated by chlorite-rich micritic limestone; (3) pale red oxidized scoriaceous basalt composed of aphanitic basaltic rocks passing gradually to a highly vesicular zone; (4) medium gray basalt containing few altered light olive gray zones enriched in opaques. The bottom of the drilled hole consists of alternating flows of highly vesicular basalt, amygdalar basalts, and patchy non-vesicular basalts.

The sediments overlying the igneous rocks at Site 216 were inferred to be deposited in a shallow-water environment. The basalts at this Site differ in composition, texture, and mineral paragenesis from typical mid-ocean ridge basalts (Bougault, 1974; Hekinian, 1974; Thompson et al., 1974). Most of the clinopyroxene and plagioclase in them are fresh, and only a small amount

of them is altered into chlorite (Hekinian, 1974). However, there are light olive gray zones with a colorless pale-brown diopside-hedenbergite in a matrix of Fe-oxyhydroxides (Hekinian, 1974). These highly altered basalts may be related to a shallow hydrothermal discharge zone with precipitation of Cu-sulfide in veins. Native copper occurs as vein filling in this localized hydrothermally altered zone.

2.3. Site 364

A thick sediment-rock sequence was drilled at Site 364 (DSDP Leg 40) with calcareous mud and clay ($N_2^3 – Q_1$), marly nannofossil ooze and mud ($N_1^2 – N_2^1$), yellow-brown pelagic clay and radiolarian mud ($Pg_3^2 – N_1^2$), yellow-brown and brown nanno chalk and marly chalk ($K_2^{st} – Pg_2^2$), chalks, marly chalks and mudstones with sapropels [$K_2^{cm}(?) – K_2^{st}$], bluish-gray to olive-gray limestone and marly limestone [$K_1^{alb}(?)$], marly dolomitic limestone with sapropel [$K_1^{apt} – K_1^{alb}(?)$] (Fig. 1; Bolli et al., 1978). It is supposed (Bolli et al., 1978) that the drilled sequence at this site covers evaporates. Within the drilled section two of the lithologic units contain carbonates or marly carbonates interbedded with black, finely laminated sapropels with up to 15% $C_{org.}$ and abundant pyrite. The native Cu occurrences are in the upper part of an oxidized sediment unit: dark yellowish-brown to olive marly nannofossil ooze at the top becoming yellowish-brown to gray pelagic clay toward the bottom. The overlaying sediment units are composed of dark olive-gray to black calcareous mud, which contain up to 4% pyrite indicating reducing conditions.

2.4. Site 597

The drilled sequence at Site 597C (DSDP Leg 92) comprises zeolitic clay, clay bearing to clayey nannofossil ooze, ash layer, olivine-bearing aphyric basalt, olivine-free basalt, and olivine-bearing basalt (Fig. 1; Leinen et al., 1986). Native Cu particles and veins occur in the basalts. The basalt has undergone incipient to moderate alteration. According to Peterson et al. (1986) there are 3 secondary mineral assemblages in the altered basalts at this Site which formed in the following order: (1) trioctahedral chlorite and talc; (2) goethite and smectite; (3) calcite and celadonite. The sequential precipitation of these mineral assemblages denotes high water/rock ratios and time-varying conditions of temperature (early >200°C to late <30°C) and state of oxidation (early nonoxidative to late oxidative). The intensity of alteration decreases with depth, probably partly as a result of a decrease in vesicularity and fracture spacing (Leinen et al., 1986). Oxidative low-temperature seawater alteration is supposed to influence the upper portion (down to 120 m below seafloor) of the basaltic basement at Site 597C (Erzinger, 1986), whereas the lowermost basement was affected by a non-oxidative hydrothermal alteration occurring at higher temperature (Nishitani, 1986).

2.5. Site 642

Drilling at Site 642E (ODP Leg 104) recovered a long core of mud (N_2 – Q), nannofossil and radiolarian ooze (N_1^3 – N_2), mud and nannofossil ooze (N_1^3), nannofossil and radiolarian ooze (N_1^2 – N_1^3), mud and radiolarian ooze (N_1^1 – N_1^2), mud with volcanic ash (Pg_2), basalts, and andesites and basalts (Fig. 1; Eldholm et al., 1987). Native Cu occurs as disseminated blebs in groundmass and in veins in fine-grained, aphyric to phyric and vesicular gray basalt with subvertical fractures filled with smectite and calcite. It is supposed (Eldholm et al., 1987) that these igneous rocks were deposited under subaerial conditions. Throughout the igneous sequence

there is a low-temperature suite of secondary minerals. Superimposed on this, there is a later, higher temperature overprint. Smectite, celadonite and calcite fill vesicles and fractures. This paragenesis may indicate a shift from nonoxygenated to oxygenated fluids. Early, low-temperature alteration of the lower series has been overprinted by later, higher temperature (100-130°C) effects.

3. Material and methods

We applied in the Integrated Ocean Drilling Program (IODP) for sediment and rock samples from all the 12 DSDP/ODP cores we were aware of that had been reported to contain native Cu occurrences (Fig. 1). Consequently, we were provided with 24 sediment and rock samples from 8 of those DSDP/ODP cores (Table 1). Preliminary descriptions of the native Cu occurrences not provided for this study from those four DSDP/ODP Sites (Fig. 1) can be found elsewhere (Kennett et al., 1975; Roberts et al., 1984; Knox, 1985; Puchelt et al., 1996).

All the sediment and rock samples were thoroughly investigated for metallic Cu particles using conventional stereo-microscope (Olympus SZ-ST). Although previously reported, we could not find any Cu^0 particles in the samples from 3 of the DSDP/ODP cores (Fig. 1; Berger and von Rad, 1972; Jenkyns, H.C., 1976; Talwani et al., 1976) and therefore our study is based on samples from 5 cores. In total, we found and analyzed 26 single Cu^0 particles from 9 discrete samples after crushing them with stainless steel hammer (Table 1). Six rock samples of those with native Cu particles were prepared as polished sections and investigated under optical microscope (Olympus BX60). Secondary electron images (SEI) and energy dispersive X-ray spectra (EDS) of native Cu occurrences were obtained on C-coated specimens using a Hitachi

S4300 scanning electron microscope (SEM) fitted with a solid state Si(Li) detector (V=8-20 kV, I=5-8 μA) using the INCA software package (Oxford Instruments).

Reflectance measurements on polished sections (two Cu^0 specimens) in the visible spectrum (400-700 nm) were performed with a Zeiss MPM800 microscope photometer system, equipped with 10x/0.20 and 32x/0.40 Glycerine Ultrafluar objectives, adjusted to give a field of measurement with diameter of 30 μm. Measurements were carried out in air and in oil (Zeiss 518C, n=1.518). The step size (equal to bandwidth) was 5 nm, and the data were corrected for parasitic-light effects and standardized against SiC (Zeiss no. 846). Vickers microhardness (H_v) was measured on three Cu^0 particles in polished sections with a Shimadzu micro hardness tester type-M (load 25 g, loading time 15 s). One big (~10x10 mm) native Cu flake [22-216-37-4 (114-117)] was analyzed by X-ray diffraction (XRD) using a Philips PW1710 diffractometer (graphite-monochromatised Cu K_α radiation, PW1830 generator, 40 kV, 40 mA, 42-95 °2θ scan, 0.02 °2θ step, 1 s/step). Peak positions were determined with the X'Pert Graphics and Identify program.

Concentrations of elements with $Z \geq 9$ (F) were acquired on carbon-coated polished sections of three Cu^0 specimens using a Cameca SX50 electron microprobe (EMP) (V=20 kV, I=12 nA, electron beam diameter of 2 μm and native Cu standard). The compositions (on natural surface) of four Cu^0 particles were analyzed with Particle Induced X-ray Emission (PIXE) and Rutherford Backscattering Spectroscopy (RBS) using 3 MeV H^+ ions. The ion beam was focused to a rectangular area (~20x30 μm) on the particle's surface. PIXE was applied with the aim to obtain the average concentrations of the elements with $Z \geq 12$ (Mg) and RBS has been used to obtain concentration depth profiles for the main elements. A Si(Li) detector (80 mm^2) was used to detect the X-rays emitted from the sample. The detector was placed outside the sample chamber for easy exchange of absorbers, but necessitating two Be windows with a total thickness of 150 μm

and a 6 mm air layer. An additional 100 µm thick Mylar absorber was used for the PIXE measurements of one sample only [22-216-37-4 (114-117)] whereas the other samples were measured without this absorber. An annular particle detector with a solid angle of about 18 msr was used to detect the backscattered ions. The PIXE spectra were fitted using the program GupixWin (Campbell et al., 2000) and the RBS spectra using the program NDF (Barradas et al., 1997). Nuclear Reaction Analysis (NRA) (^{15}N method; beam spot ≤1 mm^2) was used to obtain depth profile of H for one Cu^0 specimen [22-216-37-4 (114-117)].

Copper isotope analyses of native Cu separates and bulk rocks followed previously published methods. The samples were purified by a two stage anion exchange chromatography column using a procedure modified from that of Maréchal et al. (1999), Chapman et al. (2006), Borrok et al. (2007). After a complete digestion step in concentrated HF-HNO_3 and HCl-HNO_3 mixture, bulk rock and Cu^0 samples were dissolved in 2 mL of 6 mol/L distilled HCl in a closed beaker on a hot plate. A precise volume of this solution was then purified using anion exchange chromatography in an HCl medium (distilled grade). A 5 mL column was loaded with 1.8 mL Bio-Rad AG1-X8 anion resin 200 – 400 mesh (chloride form) which was acid cleaned with 10 mL of 2 mol/L HNO_3, 10 mL of ultrapure water and 10 mL of 0.24 mol/L HCl and finally conditioned with 5 mL of 6 mol/L HCl. Under these conditions, Cu (along with Fe) was adsorbed onto the anionic resin while the sample matrix was eluted using 5 mL of 6 mol/L HCl. Cu was then eluted (and separated from Fe) with 50 mL of 6 mol/L HCl, collected in a PTFE vial and evaporated to dryness. The residue was re-dissolved in 2-3 mL of 0.28 mol/L HNO_3 and then further diluted to form a 0.1 to 0.5 ppm Cu solution ready for isotope analysis. For basalt analysis, this purification step was repeated once as it was found that trace matrix elements and Fe remained in the first Cu fraction. Quantitative recovery of Cu through the entire chromatographic procedure was checked by calculating chemistry yield for all samples and also

by checking Cu concentration in eluted matrix solution. Yield was found to be systematically better than 98%.

Analyses of $^{65}Cu/^{63}Cu$ were carried out on a Thermo-Neptune MC-ICP-MS operating at low resolution. The samples were introduced into the plasma using a double spray quartz spray chamber system (cyclonic and double pass) and a microconcentric PFA nebulizer operating at a flow rate of about 60 μL min^{-1}. Instrumental mass bias was corrected for using Zn isotopes as an internal standard and involves simultaneous measurement of a Zn standard solution (SRM 3168a Standard Solution). Also a standard bracketing approach, which normalizes the Cu isotope ratio to the average measured composition of a standard (SRM 976) was carried out before and after each sample. Standard deviation values (1SD) were calculated according to the number of duplicates (N) executed and reported for each sample. Two internal standards, Spex solution and USGS basalt BHVO-2, were processed through the entire chemical procedure and gave $\delta^{65}Cu$ values of 0.02 ± 0.06‰ and 0.07 ± 0.06‰ (2SD), respectively. Purified Spex solution was observed to be indistinguishable from the pure unprocessed solution, whereas basalt BHVO-2 values were similar to values reported elsewhere (Moynier et al., 2010; Moeller et al., 2012). Following the same procedures we analyzed four additional ODP samples (two altered basalts, one deep-sea clay, one Mn-rich chert; Rouxel et al., 2003) for comparison.

We modeled Eh–pH Cu-phase diagrams using the Geochemist's Workbench 8.0 software based on the "thermo_minteq" database. Physical and chemical parameters used in our calculations are discussed in section **5**.

4. Results

The investigated native Cu particles were recovered from two different types of host rocks: sedimentary and igneous. The Cu^0 occurs as veinlets and small flakes scattered in the sedimentary rocks (Holes 105, 364). Cu^0 fills vesicles and branching cracks in the igneous basement rocks (Holes 216, 597C, 642E), which upon gentle opening reveal larger (up to c. 10 mm) thin Cu^0 leaves (Fig. 2A). Native Cu particles (Fig. 2B) scattered in the basalts and veins (Fig. 2C) crossing the basalts and sediments are composed of euhedral to subhedral crystals. The most common crystal forms are octahedrons (Fig. 2D) and cubes, which although often being very strongly distorted are recognisable on the surface of the Cu^0 leaves (Fig. 2E). The grains display very high metallic lustre on freshly cut surfaces (Fig. 2B, C). The surface colour is a brilliant deep rose-white (Fig. 2B, C), which darkens to „copper-red" and later to red-brown (Fig. 2A) if the polished surface is not immediately protected.

Reflectance values in air (and oil) from a representative Cu^0 grain [22-216-37-4 (114-117)] at the four wavelengths (470, 546, 589 and 650 nm) recommended by the IMA Commission on Ore Minerals are 56.7 (45.0), 64.5 (55.2), 92.0 (86.1), and 97.0 (95.6), respectively. The obtained reflectance spectra compare very well with those listed for native Cu (Fig. 3) in the Quantitative Data File for Ore Minerals (Criddle and Stanley, 1993).

Vickers microhardness (H_v) measurements on polished sections gave average values [22-216-37-4 (114-117): H_v=65.5 (10 measurements); 92-597C-4-1C (33-35): H_v=80.5 (3 measurements); 92-597C-7-3 16 (135-138): H_v=71.3 (three measurements)] similar to the data reported on other native Cu occurrences (Ramdohr, 1980).

XRD investigations of a Cu^0 leaf [22-216-37-4 (114-117)] showed characteristic reflections and a unit cell parameter [(*hkl*), $d_{obs.}$ (Å), $d_{calc.}$ (Å), relative intensity (%): (*111*), 2.077, 2.084, 100; (*200*), 1.802, 1.804, 4; (*220*), 1.276, 1.276, 75; (*311*), 1.090, 1.088, 37] (a_0=3.609 Å) comparable to those observed in diffractograms of other native copper samples [(*hkl*), d (Å),

relative intensity (%): (*111*), 2.088, 100; (*200*), 1.808, 46; (*220*), 1.278, 20; (*311*), 1.090, 17] (a_0=3.6150 Å) (Powder Diffraction File 4-836).

EMP analyses on polished sections native Cu grains revealed they were almost pure Cu [22-216-37-4 (114-117): Cu=99.3 wt.%, average of 5 analyses; 92-597C-4-2D (60-65): Cu=98.1 wt.%, average of 8 analyses], sometimes with negligible Fe concentration [92-597C-7-3 16 (135-138): Cu=98.8 wt.%, Fe=0.14 wt.%, average of 9 analyses] and traces of Sn and Ca (in a few point analyses).

The mineral phases in visible close association with the Cu^0 particles (stuck on their surface) vary in colour from light-blue to turquoise-blue (Fig. 2A). They form masses of fine granules (Fig. 2F) or needle-like crystals (Fig. 2H), clusters of kidney-like grains (Fig. 2G) and aggregates of lamellar crystals (Fig. 2F). According to the EDS studies they are copper oxy-halides (Cu, Cl, O) and copper sulphate oxy-chlorides (Cu, S, Cl, O). EMP analyses (three spots) on polished section of these mineral phases [92-597C-4-2D (60-65)] yield an average composition (in wt.%): Cu=85.1, O=14.2, Cl=1.37, Fe=0.02. PIXE analyses (Table 2) on the natural surfaces of two native Cu particles are close to the EMP results. However, the Cl and Fe contents recorded by PIXE are about an order of magnitude higher, suggesting that the native copper particles are coated with microscopic to submicroscopic surface layers of contrasting composition. The recorded traces of Si, Ca and K (Table 2) might be due to analysis of fine silicate particles adhered to the Cu^0 surface, whereas the traces of As and Mn might reflect presence of these elements in the surface coating. RBS depth profiles at the natural surfaces of two native Cu grains (Fig. 4A, B) show that this surface film (presumably alteration) has a thickness of 11-16 µm and a complex structure. It can be divided into 2 sub-layers: upper (surficial) and lower (internal). In the upper sub-layer (1-6 µm) O has the highest concentration whereas Cu and Cl have equal content (Fig. 4A, B). In the lower sub-layer (2-7 µm) Cu is the

most abundant followed by O and Cl (Fig. 4A, B). The transitions upper/lower sub-layers and lower sub-layer/pure Cu^0 mark gradual Cu increase, and O and Cl decrease (Fig. 4A, B). At the base of the lower sub-layer of one of the Cu^0 particles just above the transition to pure Cu^0 there is a Cu-O sub-sublayer (2 μm) (Fig. 4A). The NRA depth profile of H for one of these Cu^0 particles shows decrease of H content with increasing depth in the surface film: at 0.5 μm, 23.5 at.% H; at 1.0 μm, 16.8 at.% H.

The Cu isotope compositions of the two types of native Cu occurrences (sedimentary rock-hosted and igneous rock-hosted) show different trends (Table 3). Sedimentary rocks that host Cu^0 grains have slightly negative $\delta^{65}Cu$ values ($\delta^{65}Cu_{average}$ = -0.13‰, 1SD = 0.02‰, N = 4) whereas the Cu^0 grains in them show positive $\delta^{65}Cu$ values (0.4-1.0‰; Table 3). The basalts and native Cu occurrences in them have slightly positive (0.0-0.3‰) $\delta^{65}Cu$ values. However, whereas the Pacific samples (both basalt and native Cu) have $\delta^{65}Cu$ values clustering at 0.0‰, the samples from the Indian Ocean show slight enrichment in heavy isotopes with $\delta^{65}Cu_{basalt}$ = 0.3‰ and $\delta^{65}Cu_{native\ Cu}$ = 0.1-0.2‰ (Table 3). The reference altered basalts ($\delta^{65}Cu_{average}$ = 0.05‰, 1SD = 0.03‰, N = 4) and deep-sea clays ($\delta^{65}Cu_{average}$ = 0.01‰, 1SD = 0.02‰, N = 4) from other ODP sites have Cu isotope compositions close to the average crustal value: $\delta^{65}Cu$ = 0.0-0.1‰ (Table 3).

5. Discussion

The studied native Cu occurrences are hosted in two types of rocks: igneous and sedimentary. These two different geologic associations imply different mechanisms of native Cu formation and possibly different Cu sources. In general, Cu^0 occurs in a wide variety of environments (basic and ultrabasic igneous rocks, sedimentary rocks and sulfide ores) and

obviously forms via a range of processes (Cornwall, 1956), which explains the number of genetic models proposed for any particular native Cu deposit.

5.1. Cu isotope systematic and native Cu formation in volcanic basement

5.1.1. Primary magmatic origin

Based on theoretical considerations and experimental studies, it has already been suggested that native Cu in basalt may have a primary magmatic origin (Hofmeister and Rossman, 1985; Cabral and Beaudoin, 2007). The magmatic origin of Cu^0 supposes it has crystallized in equilibrium with the basaltic magma. Investigations of the Cu-isotope composition of primary Cu^0 grains in ultramafic rocks (Ikehata and Hirata, 2012) showed homogeneous $\delta^{65}Cu$ values between −0.03 and 0.14‰, implying that there is no significant Cu-isotope fractionation during high-temperature magmatic processes. Studies on magmatic Cu^0 (Cabral and Beaudoin, 2007) revealed that it occurs as micrometric (~50 µm) inclusions in rock-forming minerals and contains high concentrations of volatile elements (0.2-2.0% S, up to 0.6% As). However, the native Cu from Site 597C occurs mainly as vein fillings and does not have EMP detectable (≥0.1 wt.%) content of S and As. This suggests that these Cu^0 occurrences are not primary magmatic although they have $\delta^{65}Cu$ values close to that of the host basalt (~0.0‰, Table 3).

5.1.2. Secondary formation through low-temperature in situ *alteration of Cu-sulfides*

In seafloor basalts, the primary (magmatic) Cu-mineral is chalcopyrite (Gitlin, 1985). In addition, hydrothermal fluid circulation at mid-oceanic ridges leads to alteration of the basement rocks with precipitation of Cu-sulfides as disseminated mineralization in veins (Dill et al., 1992; Alt, 1995; Teagle and Alt, 2004; Sharkov et al., 2007). Although no evidences of both magmatic

and hydrothermal Cu-sulfides could be identified throughout the basement section where we studied native Cu, some sections (e.g., of Site 216) clearly show evidence for hydrothermal alteration. Therefore, we cannot theoretically rule out the possibility that native Cu has formed as secondary product of *in situ* chalcopyrite alteration.

Supergene alteration of the chalcopyrite ($Cu^{+}Fe^{3+}S_2^{2-}$; Pearce et al., 2006) may proceed through the following reaction:

$$2Cu^{+}Fe^{3+}S_2 + 8O_{2(aq)} + 2H^{+} \leftrightarrow 2Cu^{+} + Fe_2(SO_4)_3 + H_2SO_4 \quad \text{(Reaction 1)}$$

This reaction goes towards chalcopyrite dissolution as Eh increases and pH decreases. Released Cu^{+} may further be reduced to Cu^{0} by the action of ferric sulfate:

$$Cu^{+} + Fe_2(SO_4)_3 + 2H^{+} + 3e^{-} \leftrightarrow Cu^{0} + 2FeSO_4 + H_2SO_4 \quad \text{(Reaction 2)}$$

Although Cu-isotope fractionation factors for reaction 2 are not known from experimental studies, it has generally been considered that native Cu formation through this process may lead to significant Cu-isotope fractionation (Larson et al., 2003; Ikehata et al., 2011). The direction of Cu-isotope fractionation, however, is unclear. Larson et al. (2003) have suggested that Cu^{+} reduction to Cu^{0} in hydrothermal conditions may lead to higher Cu-isotope values during precipitation of native Cu, whereas Ikahata et al. (2011) reported lower $\delta^{65}Cu$ values for secondary native Cu. In addition, Cu-isotope fractionation may also proceed during the leaching of Cu-sulfides (reaction 1), with a preferential release of heavier Cu-isotope (Rouxel et al., 2004; Kimball et al., 2009). Hence, considering the restricted range of Cu-isotope fractionation in Cu^{0} recovered in volcanic basement, it is unlikely that native Cu form during supergene *in situ* alteration of magmatic and hydrothermal Cu-sulfides.

5.1.3. Direct precipitation during low-temperature ridge flank fluid circulation

In addition to the main primary Cu-mineral in seafloor basalts (chalcopyrite) Cu also occurs as trace element in primary magmatic Fe-sulfides and silicates (e.g., olivine, basaltic glass) in the basement rocks. Seafloor weathering of basaltic glass (palagonitization) results in ~25% depletion of Cu relative to the unaltered glass (Ailin-Pyzik and Sommer, 1981). This suggests that low-temperature alteration of the basaltic glass by seawater may be a source of Cu to the resultant fluid. Therefore, the dissolution of primary minerals (sulfides, olivine) and volcanic glass during basalt alteration by seawater might be considered as a principal process supplying Cu to the mineralizing fluid. Low-temperature seawater-basalt interaction leads to pervasive oxidation of primary magmatic sulfides (chalcopyrite, pyrrhotite) and breakdown of primary igneous silicates with formation of secondary oxyhydroxides, sulfates and clays (Alt, 1995; Bach and Edwards, 2003). Low-temperature oceanic basement alteration is a ubiquitous process that occurs at vast areas at mid-ocean ridge (MOR) flanks (affects >1/3 of the seafloor), where convection of seawater in the crust persists for several tens of millions of years (Wheat et al., 2000; 2003). In order to determine whether low-temperature seawater-basalt interactions may lead to the formation of native Cu in the oceanic basement, we modeled Eh-pH phase diagrams using the compositional parameters of fluids encountered at mid-ocean ridge flank setting. Based on the investigation of the pore fluids extracted from the sediment above the oceanic basement and diffuse vent fluids at the seafloor Wheat and Mottl (2000) and Wheat et al. (2000; 2002) inferred the chemical composition of the basement fluids (formation waters) and chemical fluxes during basement alteration. These fluids are of two types: “cool” (20-25°C) and “warm” (60-65°C) (Wheat et al., 2003) with Cu concentrations of 2 and 0.2 nmol/L, respectively. These contents are lower than that of the deep seawater (5.6 nmol/L) entering the crust and imply that the oceanic crust acts as a sink for Cu from the seawater. In fact the model of Wheat et al. (2002; 2003) presents data from the beginning (seawater) and end (vent fluid) of the circulation cell. In

the absence of data for the circulation cell between these two end points, we suppose that a complex scenario forms the basement fluid composition. Therefore, we may speculate that low-temperature alteration of the oceanic crust supplies Cu to the basement fluids through breakdown of Cu-containing minerals. Copper leached from the crust dominates over seawater Cu in the Cu budget of the basement fluids. During basement fluid circulation major part of dissolved Cu (leached + seawater Cu) reprecipitates in the crust and does not enter the ocean with the "cool" and "warm" vent fluids.

Our initial calculations showed that in the temperature range 20-65°C the stability fields of different Cu species do not change significantly. Therefore, we report the Eh-pH diagrams at 60°C (Fig. 5). Since we are not able to estimate the local Cu concentration in the basement fluids at the point of Cu leaching from the primary minerals, we have taken the seawater Cu activity value ($a[Cu] = 5.6\ 10^{-9}$, calculated from [Cu] = 5.6 nmol/L) in our modeling (Fig. 5). The activities of other components used in the modeling ($a[Cl] = 0.55$; $a[S] = 0.018$; $a[Fe] = 1\ 10^{-9}$) were calculated from their concentrations in the basement fluids reported by Wheat et al. (2010). Since the effect of pressure on the calculations in the relevant range of shallow burial is negligible, all calculations were made under standard state pressure of 1 atm.

The stability fields of Cu- and Fe-sulfides at low-temperature (20-65°C) in the oceanic basement (Fig. 5a, b) are controlled by the activity of H_2S or HS^- (Fig. 5c). Cu^0 is stable under low Eh and high pH conditions when H_2S and/or Fe are absent (Eh<-0.25 V; pH>5; Fig. 5a, d, e) and practically cannot exist in the system Fe-Cu-S. In anoxic basalt-dominated systems absence of Fe^{2+} in solution is unlikely, but not the absence of H_2S. Such conditions may prevail during low-temperature basalt alteration where the dissolution of olivine and volcanic glass at low water/rock ratios generate Fe^{2+} in solution without thermogenic seawater sulfate reduction (Seyfried and Bischoff, 1979). Fig. 5e is calculated for such a system. It is important to note that

every increase in a[Cu] or a decrease of a[Cl] will expand the stability field of the Cu^0. When H_2S is present (Fig. 5a) and assuming H_2S/SO_4 equilibrium conditions, Cu-sulfide minerals become more dominant in the low Eh range and the stability field of Cu^0 shrinks to relatively basic (pH>9) conditions, or completely disappears when Fe^{2+} is present in solution (Fig. 5b).

Since the stability field of the Cu^0 overlaps with the stability field of Cu^+ species, it is assumed that Cu^0 is precipitated directly from Cu^+ species in such reaction:

$$4CuCl_2^- + 2H_2O \leftrightarrow 4H^+ + O_{2aq} + 4Cu^0{}_{metal} + 8Cl^- \quad \text{(Reaction 3)}$$

Copper isotope fractionation factors for such a reaction are not known (Fujii et al., 2013). Because reduction of metals typically produces negative fractionations (Ellis et al., 2002; Ehrlich et al., 2004; Tossell, 2005), similar fractionation trend could be expected for the process of Cu^0 precipitation from Cu^+-bearing solution (Reaction 3).

Basalts and Cu^0 from Sites 216 and 597C show $\delta^{65}Cu$ values of 0.30 and 0.07 ‰, and 0.14-0.19 and 0.02 ‰, respectively (Table 3). The fact that all basalt samples fall within the igneous rocks $\delta^{65}Cu$ range [~0‰ (Zhu et al., 2000; Larson et al., 2003; Mason et al., 2005; Mathur et al., 2005; Asael et al., 2007; Moynier et al., 2010; Moeller et al., 2012)] shows that no significant processes of Cu-isotope fractionation occurred in them during and after the formation of the Cu^0, probably due to the fact that bulk Cu concentration in the rocks is not greatly affected by alteration processes. Cu-isotope composition of altered basalts from ODP Sites 801 and 1149 (Table 3) also confirm the lack of Cu-isotope fractionation during seafloor weathering.

At Site 216, the host basalt is anomalously enriched in Cu ([Cu] > 2000 ppm), but this enrichment is probably due to disseminated Cu^0 grains within the rock groundmass. The fact that significant quantity of Cu is found enriched in veins and even in bulk rock suggests that Cu should have been mobilized from large volume of volcanic rock before being concentrated

locally. This requires considerable migration of Cu-bearing solutions together with an efficient trapping mechanism.

In the altered oceanic crust, the buffered pH conditions due to seawater/rock reactions, low Eh due to Fe^{2+} release from the basalt and absence of sulfate reduction would result in conditions suitable for Cu^0 precipitation (Fig. 5). Cu-bearing solutions within the oceanic crust are likely to form during low-temperature alteration of basement rocks through interaction with seawater and breakdown of Cu-containing minerals. Although Wheat et al. (2002; 2003) suggested that oceanic crust alteration via interaction with seawater may provide a net sink of seawater Cu, our Cu-isotope data for native Cu argue against a seawater origin of Cu, since (1) $\delta^{65}Cu_{seawater}$ = +0.8 – +1.5‰ (Vance et al., 2008; Takano et al., 2013; Thompson et al., 2013) and (2) reduction of Cu^{2+}, which is the main redox Cu species in seawater, to Cu^+ and ultimately to Cu^0 would produce large range of Cu-isotope composition depending on the extent of reduction (Ehrlich et al., 2004; Mathur et al., 2005). Hence, the limited Cu-isotope fractionation found in basalt-hosted Cu^0 has likely resulted from the transport of Cu mainly as Cu^+ species. It also suggests limited Cu-isotope fractionation during Cu leaching from the basement rocks (e.g., glass, sulfides and silicates).

Finally, we suggest that the Cu^0 occurrences in the basalts can only form under low a[Cu] and H_2S conditions precluding the precipitation of Cu^+-secondary minerals. The precipitation of Cu^0 would have proceeded over protracted periods as the alteration fluids (basement fluids) circulate through basalt fractures. It is further possible that Cu^0 precipitation in veins has resulted from autocatalytic reaction or at specific redox front within the rock under low Eh condition and where H_2S is absent or very low.

5.2. Isotope constraints of Cu source and native Cu formation in marine sediments

Sedimentary rocks hosting native Cu at Sites 105 (clayey reddish-brown limestone) and 364 (yellowish brown pelagic clay) have slightly negative δ^{65}Cu values (-0.06 and -0.19‰, respectively) that differ from that of the average deep-sea clays (0.01‰) (Table 3). However, the Cu^0 occurrences in them show heavier Cu-isotope composition: 0.41-0.49‰ and 0.95‰, respectively.

At Site 105, native Cu is located within well lithified red clayey limestones ~10 m above the basement. The red color of the host rocks is due to hematite staining (Lancelot et al., 1972) that may have been derived from Fe-oxyhydroxides syngenetically precipitated from seawater as a result of hydrothermal input. Hence, the Cu source in these sedimentary rocks might be related to seafloor hydrothermal activity such as plume fallout containing Cu-sulfides [chalcopyrite, cubanite, covellite; Mottl and McConachy (1990)].

At Site 364, native Cu is located within a thick sediment layer of marly ooze and pelagic clay, ~3000 m above the sediment/basement interface. Although the ultimate Cu source is unclear, Cu enrichment is likely authigenic: either through direct Cu precipitation from seawater (co-precipitation with Fe-Mn-oxyhydroxides or adsorbed on them; i.e., hydrogenetic), oxidation of organic matter, or eventually from hydrothermal plume fallout (Cu-sulfides or Cu^{2+} scavenged from seawater by Fe-oxyhydroxides). The lack of Mn and Ni enrichment associated with Cu^0 occurrence requires specific diagenetic reactions that would explain both the precipitation of Cu^0 and lack of other metal enrichments that are typical of hydrogeneous precipitates.

It is important to note that seawater shows positive δ^{65}Cu values: 0.8 – 1.5‰ (Bermin et al., 2006; Vance et al., 2008; Takano et al., 2013; Thompson et al., 2013). Hydrogeneous Mn-Fe-oxyhydroxide nodules are also characterized by positive δ^{65}Cu values: 0.1 – 0.6‰ (Albarède, 2004). In addition, experimental studies of Cu^{2+} adsorption onto amorphous Fe^{3+}-oxyhydroxides

suggest an enrichment of heavy Cu isotope in the solid phase (Balistrieri et al., 2008; Pokrovsky et al., 2008). Hence, from an isotopic point of view, seawater is a likely Cu source for the Cu^0 occurrence in the sediments. A two-stage process may explain both positive $\delta^{65}Cu$ values and native Cu formation. First, hydrogeneous and/or hydrothermal enrichment of Cu through adsorption onto Mn-Fe-oxyhydroxides leads to the formation of isotopically heavy Cu reservoir in the sediment. During early diagenetic remineralization of organic matter in the sediment, anaerobic microbial respiration would reduce Mn- and Fe-oxyhydroxides and result in a net loss of those metals (and others) to the seawater/sediment interface. Organic matter remineralization through microbial processes may also provide reduction mechanisms to generate Cu^0 from Cu^{2+}. In that case, complete reduction of Cu^{2+} to Cu^0 would preserve its original isotope signature, which is in this case characterized by positive $\delta^{65}Cu$ values. The relatively low concentrations of organic matter at Sites 105 and 364 would also result in very limited sulfate reduction in porewaters, therefore precluding the precipitation of Fe-Cu-sulfides instead of native Cu.

Cu-isotope data for the visible bluish phases on the Cu^0 surfaces ($\delta^{65}Cu_{bluish\ phase} < \delta^{65}Cu_{native\ Cu}$; Table 3) may give further clues to their origin. The composition (EMP data on polished section) of these phases is close to those of atacamite and paratacamite. Whereas some native Cu particles had such minerals visibly stuck on their surfaces other Cu^0 grains exhibited clear surfaces without any visible mineral phases on them. With PIXE we targeted this type of clear surfaces of native Cu particles and likely the PIXE data represent the composition of a thin, surface alteration film of Cu^0. The visible mineral phases (EMP analyses) on the Cu^0 surfaces may form not only as alteration products, but might also be minerals precipitated contemporarily or after the Cu^0 formation. Although the composition of the surface film of Cu^0 particles (PIXE data) does not match precisely the composition of any mineral phase, these data along with the

RBS and NRA depth profiles suggest that the surface alteration film is composed of phases very close to atacamite and paratacamite. This sounds reasonable in view of stability and mode of formation of these minerals at seafloor conditions (Hannington, 1993). The complex structure of this surface film (composed of sub-layers of different composition) implies that the alteration of native Cu at seafloor conditions is a process dependant on the kinetics of reactions of Cu^0 with pore fluid O_2 and Cl^-. The composition of the surface film sub-layers suggests an evolution of the alteration phase from oxygen-dominated copper oxy-chloride (surficial sub-layer) towards atacamite/paratacamite-like phase (internal sub-layer).

The $\delta^{65}Cu$ values of the bluish Cu^{2+}-phases around the Cu^0 grains are between those of the host rock and of the Cu^0. Oxidation of Cu is accompanied by positive isotope fractionation (Rouxel et al., 2004; Mathur et al., 2005; Asael et al., 2007). A simple oxidation process of the Cu^0 grains can explain the fact that the isotopic composition of the Cu^{2+}-phases is heavier with respect to the Cu^0 grains. Precipitation of atacamite and paratacamite (Cu^{2+}-minerals that compose the bluish phases) requires a[Cu] values in the solution which are at least an order of magnitude higher than that necessary for Cu^0 precipitation (Eh-pH phase diagram not shown). In addition, OH^- should also be available in the system. Hence, the most likely source for the high a[Cu] values in the fluid is local partial re-dissolution of the Cu^0 grains.

5.3. Comparison with economic-size native Cu deposits

Native Cu deposits are amongst the most important Cu resources (e.g., Wang et al., 2006; Cooper et al., 2008; Pinto et al., 2011). Generally, they are interpreted to be genetically related to the associated magmatic rocks despite the low Cu concentrations in magmatic systems (Cornwall, 1956; Amstutz, 1977). A major question that remains debatable is the mechanism that effectively

mobilizes Cu from a Cu-poor matrix and eventually concentrates it in economic grades. Therefore, it is not surprising that a number of scenarios have been proposed for the origin of native Cu deposits (e.g., Cornwall, 1956; Brown, 2006). A general issue of all the genetic models is that a detailed investigation of the mechanisms of Cu mobilization, concentration and deposition is limited because once the Cu-deposit has formed pre-ore host-rock Cu contents and concentration mechanisms are no longer accessible. Later processes additionally obscure the situation and complicate the deciphering of the original conditions. Therefore, Cu^0 occurrences disseminated in the oceanic crust present an opportunity to investigate Cu-isotope signatures of native Cu in a pre-ore setting and to eventually use them in further genetic models of native Cu deposits.

In this context it would be interesting to compare the Cu-isotope composition of Cu^0 from the oceanic crust with that of Cu^0 from the native Cu deposits. Copper isotope composition of native Cu occurrences from continental ore deposits (Table 4) shows a range of ~5‰: $\delta^{65}Cu$ = -3.03 – +2.0‰. The broadest range of Cu-isotope variations is for supergene Cu^0 ($\delta^{65}Cu$ = -3.03 – +1.71‰), whereas the hydrothermal Cu^0 exhibits less Cu-isotope variations ($\delta^{65}Cu$ = -1.3 – +1.25‰) (Table 4). There is no clear isotopic difference between different genetic types of native Cu. Native Cu from the oceanic crust (Table 3) shows only positive Cu-isotope values ($\delta^{65}Cu$ = 0.02 - 0.95‰) and a much narrower range of Cu-isotope variation. Our data (Table 3) and interpretations also show that Cu^0 of similar Cu-isotope composition may have different modes of formation. Another important finding of our study is that the restricted range of $\delta^{65}Cu_{native\ Cu}$ clustered around igneous rocks isotope values does not necessarily mean a primary (magmatic) origin of Cu^0.

6. Conclusions

Precipitation of native Cu is a minor yet ubiquitous process in the sedimentary and igneous sections of the oceanic crust. Using Cu isotope systematic, we showed that primary magmatic Cu-containing minerals (sulfides, silicates, volcanic glass), hydrothermal Cu-sulfides and seawater were potential sources of Cu in this environment. Overall, within the basaltic basement, Cu dissolution and Cu^0 precipitation occurred in conditions where Cu^+-species were dominant, Cu redox fractionation did not take place and this resulted in relatively small Cu-isotope variations. On the other hand, it seems that the larger Cu-isotope variations observed in the Cu^0 in the sedimentary rocks reflect solutions, which were generally dominated by seawater-derived Cu^{2+}-species that underwent redox processes during the diagenesis leading to precipitation of Cu^0 with larger Cu-isotope fractionation.

Cu^0 formation in the basaltic basement is related to seawater-rock interaction at ridge flank setting that results in low-temperature (20°-65°C) hydrothermal activity (Fig. 6). Following the model by Wheat et al. (2002) we presume that cold and oxic seawater enters the crust at MOR crest, alters (warms and becomes anoxic) during its flow within the crust and vents out the seafloor (at discharge zones). Evidences suggest that the basement fluid may progressively loose only a small fraction of SO_4^{2-} as a result of diffusive exchange with the overlying anoxic and organic-rich sediment (cf. Elderfield et al., 1999) or microbial sulfate reduction (Rouxel et al., 2008; Ono et al., 2011). The evolving anoxic, but H_2S-deficient fluid creates favorable conditions for Cu discharge and Cu^0 precipitation. Sediment cover receives major Cu contribution from hydrogenous and hydrothermal (plume fallout) sources. Disseminated hydrogenous and/or hydrothermal Cu might be diagenetically remobilized and eventually reprecipitated as Cu^0 in reducing microenvironment.

Although the Cu^0 occurrences in the oceanic crust are unusual they apparently are not very rare. The fact that they are rarely reported in the DSDP/ODP cores likely means that they may have often been overlooked. Despite the scarcity and microscopic scale of Cu^0 occurrences the results of our investigation gave some clues on Cu sources and Cu^0 deposition at an early stage before its concentration in large deposits of economic grade.

Several major questions remain open for future studies: (1) what are the Cu fractionation factors during Cu^0 precipitation and Cu^0 oxidation (to be theoretically and experimentally tackled); (2) what proportion of Cu is as Cu^0 in the host rock, what is the Cu redox budget (Cu^0 : Cu^+ : Cu^{2+}) of the rocks and which minerals host Cu^+ and Cu^{2+}; (3) is the oceanic crust sink or source of Cu for the overlaying ocean, or it has a dual function (sink and source); (4) can the insights gained might be extrapolated to other metals, which show similar geochemical behavior: e.g., Zn and its rare occurrence as native Zn (Clark and Sillitoe, 1970)?

Acknowledgements

We express our gratitude to the IODP for providing the sample material. This study was supported by AIM (Centre for Application of Ion Beams to Materials Research, Research Infrastructures Transnational Access Contract #025646), WHOI Mary Sears program (#27002735), SYNTHESYS (grant SE-TAF-4976; EC Research Infrastructure Action, FP6 Structuring the European Research Area) and Marie Curie Intra European Fellowship (7th European Community Framework Programme; grant #253182, IsoBAB) grants, which are greatly appreciated. This article has been much improved following the reviews by R. Mathur and D. Canil.

References

Abrajano, T.A., Pasteris, J.D., 1989. Zambales ophiolite, Philippines. II. Sulfide petrology of the critical zone of the Acoje Massif. Contrib. Mineral. Petrol. 103, 64-77.

Ailin-Pyzik, I.B., Sommer, S.E., 1981. Microscale chemical effects of low temperature alteration of DSDP basaltic glasses. J. Geophys. Res. 86 (B10), 9503-9510.

Albarède, F., 2004. The stable isotope geochemistry of copper and zinc. Rev. Mineral. Geochem. 55, 409-427.

Alt, J.C., 1995. Sulfur isotopic profile through the oceanic crust: Sulfur mobility and seawater-crustal sulfur exchange during hydrothermal alteration. Geology 23, 585-588.

Amstutz, G.C., 1977. Time- and strata-bound features of the Michigan copper deposits (USA). In: Klemm, D.D., Schneider, H.-J., (Eds.), Time- and Strata-Bound Ore Deposits, Springer, Berlin-Heidelberg, 123-140.

Anbar, A.D., Rouxel, O., 2007. Metal stable isotopes in paleoceanography. Annu. Rev. Earth Planet. Sci. 35, 717-746.

Asael, D., Matthews, A., Bar-Matthews, M., Halicz, L., 2007. Copper isotope fractionation in sedimentary copper mineralization (Timna Valley, Israel). Chem. Geol. 243, 238-254.

Asael, D., Matthews, A., Oszczepalski, S., Bar-Matthews, M., Halicz, L., 2009. Fluid speciation controls of low temperature copper isotope fractionation applied to the Kupferschiefer and Timna ore deposits. Chem. Geol. 262, 147-158.

Bach, W., Edwards, K.J., 2003. Iron and sulfide oxidation within the basaltic ocean crust: Implications for chemolithoautotrophic microbial biomass production. Geochim. Cosmochim. Acta 67, 3871-3887.

Bai, W., Robinson, P.T., Fang, Q., Yang, J., Yan, B., Zhang, Z., Hu, X.-F., Zhou, M.-F., Malpas, J., 2000. The PGE and base-metal alloys in the podiform chromitites of the Luobusa ophiolite, southern Tibet. Can. Mineral. 38, 585-598.

Balistrieri, L.S., Borrok, D.M., Wanty, R.B., Ridley, W.I., 2008. Fractionation of Cu and Zn isotopes during adsorption onto amorphous Fe(III) oxyhydroxide: Experimental mixing of acid rock drainage and ambient river water. Geochim. Cosmochim. Acta 72, 311-328.

Barradas, N.P., Jeynes, C., Webb, R.P., 1997. Simulated annealing analysis of Rutherford backscattering data. Appl. Phys. Lett. 71, 291-293.

Berger, W.H., von Rad, U., 1972. Cretaceous and Cenozoic sediments from the Atlantic Ocean. In: Hayes, D.E., Pimm, A.C., et al. (Eds.), Init. Repts. DSDP. Washington (U.S. Govt. Printing Office), 14, 787-954.

Bermin, J., Vance, D., Archer, C., Statham, P., 2006. The determination of the isotopic composition of Cu and Zn in seawater. Chem. Geol. 226, 280-297.

Bolli, H.M., Ryan, W.B.F., Foresman, J.B., Hottman, W.E., Longoria, J.F., McKnight, B.K., Natland, J., Proto-Decima, F., Siesser, W.G., 1978. Angola Continental Margin-Sites 364 and 365. In: Bolli, H.M., Ryan, W.B.F., et al. (Eds.), Init. Repts. DSDP. Washington (U.S. Govt. Printing Office), 40, 357-455.

Borrok, D., Wanty, R.B., Ridley, W.I., Wolf, R., Lamothe, P.J., Adams, M., 2007. Separation of copper, iron, and zinc from complex aqueous solutions for isotopic measurement. Chem. Geol. 242, 400-414.

Borrok, D., Nimick, D., Wanty, R., Ridley, W., 2008. Isotopic variations of dissolved copper and zinc in stream waters affected by historical mining. Geochim. Cosmochim. Acta 72, 329-344.

Bougault, H., 1974. Distribution of first series transition metals in rocks recovered during DSDP Leg 22 in the northeastern Indian Ocean. In: von der Borch, C.C., Sclater, J.G., et al. (Eds.), Init. Repts. DSDP. Washington (U.S. Govt. Printing Office), 22, 213-265.

Brown, A.C., 2006. Genesis of native copper lodes in the Keweenaw district, northern Michigan: A hybrid evolved meteoric and metamorphogenic model. Econ. Geol. 101, 1437-1444.

Cabral, A.R., Beaudoin, G., 2007. Volcanic red-bed copper mineralisation related to submarine basalt alteration, Mont Alexandre, Quebec Appalachians, Canada. Miner. Deposita 42, 901-912.

Campbell, J.L., Hopman, T.L., Maxwell, J.A., Nejedly, Z., 2000. The Guelph PIXE software package III: Alternative proton database. Nucl. Instrum. Meth. B 170, 193-204.

Chapman, J.B., Mason, T.F.D., Weiss, D.J., Coles, B.J., Wilkinson, J.J., 2006. Chemical separation and isotopic variations of Cu and Zn from five geological reference materials. Geostand. Geoanal. Res. 30, 1-12.

Clark, A.N., Sillitoe, R.H., 1970. Native zinc and α-Cu,Zn from mina Dulcinea de Llampos, Copiapó, Chile. Am. Mineral. 55, 1019-1021.

Cooper, H.K., Duke, M.J.M., Simonetti, A., Chen, G.C., 2008. Trace element and Pb isotope provenance analyses of native copper in northwestern North America: results of a recent pilot study using INAA, ICP-MS, and LA-MC-ICP-MS. J. Archaeol. Sci. 35, 1732-1747.

Cornwall, H.R., 1956. A summary of ideas on the origin of native copper deposits. Econ. Geol. 51, 615-631.

Cowen, J.P., Giovannoni, S.J., Kenig, F., Johnson, H.P., Butterfield, D.A., Rappe, M.S., Hutnak, M., Lam, P., 2003. Fluids from aging ocean crust that support microbial life. Science 299, 120-123.

Criddle, A.J., Stanley, C.J., 1993. Quantitative Data File for Ore Minerals, 3rd ed. Chapman and Hall, London.

Dekov, V.M., Damyanov, Z.K., Kamenov, G.D., Bonev, I.K., Bogdanov, K.B., 1999. Native copper and α-copper-zinc in sediments from the TAG hydrothermal field (Mid-Atlantic Ridge, 26^{o}N): nature and origin. Mar. Geol. 161, 229-245.

Dill, H.G., Gauert, C., Holler, G., Marchig, V., 1992. Hydrothermal alteration and mineralization of basalts from the spreading zone of the East Pacific Rise (7°S - 23°S). Geologische Rundschau 81, 717-728.

Edwards, K.J., Bach, W., Rogers, D., 2003. Geomicrobiology of the ocean crust: A role for chemoautotrophic Fe-bacteria. Biol. Bull. 204, 180-185.

Ehrlich, S., Butler, I., Halicz, L., Rickard, D., Oldroyd, A., Matthews, A., 2004. Experimental study of the copper isotope fractionation between aqueous Cu(II) and covellite, CuS. Chem. Geol. 209, 259-269.

Elderfield, H., Wheat, C.G., Mottl, M.J., Monnin, C., Spiro, B., 1999. Fluid and geochemical transport through oceanic crust: A transect across the eastern flank of the Juan de Fuca Ridge. Earth Planet. Sci. Lett. 172, 151-169.

Eldholm, O., Thiede, J., Taylor, E., Barton, C., Bjørklund, K., Bleil, U., Ciesielski, P., Desprairies, A., Donnally, D., Froget, C., Henrich, R., Jansen, E., Krissek, L., Kvenvolden, K., LeHuray, A., Love, D., Lysne, P., McDonald, T., Mudie, P., Osterman, L., Parson, L., Phillips, J., Pittenger, A., Qvale, G., Schöharting, G., Viereck, L., 1987. Site 642: Norwegian Sea. In: Eldholm, O., Thiede, J., Taylor, E., (Eds.), Proc. Init. Repts. (Pt. A), ODP. 104, 53-453.

Ellis, A.S., Johnson, T.M., Bullen, T.D., 2002. Chromium isotopes and the fate of hexavalent chromium in the environment. Science 295, 2060-2062.

Erzinger, J., 1986. Basement geochemistry, Leg 92. In: Leinen, M., Rea, D.K., et al. (Eds.), Init. Repts. DSDP. Washington (U.S. Govt. Printing Office), 92, 471-480.

Fisher, A.T., Becker, K., 2000. Channelized fluid flow in oceanic crust reconciles heat-flow and permeability data. Nature 403, 71-74.

Fisk, M.R., Giovannoni, S.J., Thorseth, I.H., 1998. The extent of microbial life in volcanic crust of the ocean basins. Science 281, 978-980.

Fujii, T., Moynier, F., Abe, M., Nemoto, K., Albarède, F., 2013. Copper isotope fractionation between aqueous compounds relevant to low temperature geochemistry and biology. Geochim. Cosmochim. Acta 110, 29-44.

Furnes, H., Staudigel, H., 1999. Biological mediation in ocean crust alteration: How deep is the deep biosphere. Earth Planet. Sci. Lett. 166, 97-103.

Gitlin, E., 1985. Sulfide remobilization during low temperature alteration of seafloor basalt. Geochim. Cosmochim. Acta 49, 1567-1579.

Gold, T., 1992. The deep, hot biosphere. Proc. Natl. Acad. Sci. USA 89, 6045-6049.

Graham, S., Pearson, N., Jackson, S., Griffin, W., O'Reilly, S.Y., 2004. Tracing Cu and Fe from source to porphyry: in situ determination of Cu and Fe isotope ratios in sulfides from the Grasberg Cu-Au deposit. Chem. Geol. 207, 147-169.

Hannington, M.D., 1993. The formation of atacamite during weathering of sulfides on the modern seafloor. Can. Mineral. 31, 945-956.

Hannington, M.D., Thompson, G., Rona, P.A., Scott, S.D., 1988. Gold and native copper in supergene sulfides from the Mid-Atlantic Ridge. Nature 333, 64-66.

Hayes, D.E., Pimm, A.C., Beckmann, J.P., Benson, W.E., Berger, W.H., Roth, P.H., Supko, P.R., von Rad, U., 1972. Site 141. In: Hayes, D.E., Pimm, A.C., et al. (Eds.), Init. Repts. DSDP. Washington (U.S. Govt. Printing Office), 14, 217-247.

Hekinian, R., 1974. Petrology of igneous rocks from Leg 22 in the northeastern Indian Ocean. In: von der Borch, C.C., Sclater, J.G., et al. (Eds.), Init. Repts. DSDP. Washington (U.S. Govt. Printing Office), 22, 213-265.

Hofmeister, A.M., Rossman, G.R., 1985. Exsolution of metallic copper from Lake County labradorite. Geology 13, 644-647.

Hollister, C.D., Ewing, J.I., Habib, D., Hathaway, J.C., Lancelot, Y., Luterbacher, H., Paulus, F.J., Poag, C.W., Wilcoxon, J.A., Worstell, P., 1972. Site 105: Lower continental rise hills. In: Hollister, C.D., Ewing, J.I., et al. (Eds.), Init. Repts. DSDP. Washington (U.S. Govt. Printing Office), 11, 219-312.

Ikehata, K., Hirata, T., 2012. Copper isotope characteristics of copper-rich minerals from the Horoman peridotite complex, Hokkaido, northern Japan. Econ. Geol. 107, 1489-1497.

Ikehata, K., Notsu, K., Hirata, T., 2008. *In situ* determination of Cu isotope ratios in copper-rich materials by NIR femtosecond LA-MC-ICP-MS. J. Anal. At. Spectrom. 23, 1003-1008.

Ikehata, K., Notsu, K., Hirata, T., 2011. Copper isotope characteristics of copper-rich minerals from Besshi-type volcanogenic massive sulfide deposits, Japan, determined using a femtosecond LA-MC-ICP-MS. Econ. Geol. 106, 307-316.

Jenkyns, H.C., 1976. Sediments and sedimentary history of the Manihiki Plateau, south Pacific Ocean. In: Schlanger, S.O., Jackson, E.D., et al. (Eds.), Init. Repts. DSDP. Washington (U.S. Govt. Printing Office), 33, 873-890.

Johnson, C.M., Beard, B.L., Albarède, F., 2004. Geochemistry of Non-traditional Stable Isotopes. Reviews in Mineralogy and Geochemistry. Mineralogical Society of America; St. Louis, Washington.

Kennett, J.P., Houtz, R.E., Shipboard Scientific Party, 1975. Site 282. In: Kennett, J.P., Houtz, R.E., et al. (Eds.), Init. Repts. DSDP. Washington (U.S. Govt. Printing Office), 29, 317-363.

Kimball, B.E., Mathur, R., Dohnalkova, C., Wall, J., Runkel, R.L., Brantley, S.L., 2009. Copper isotope fractionation in acid mine drainage. Geochim. Cosmochim. Acta 73, 1247-1263.

Knox, R.W.O'B., 1985. Note on the occurrence of native copper in Tertiary nannofossil oozes from the Goban Spur (Hole 550). In: de Graciansky, P.C., Poag, C.W., et al. (Eds.), Init. Repts. DSDP. Washington (U.S. Govt. Printing Office), 80 (2), 851-852.

Lancelot, Y., Hathaway, J.C., Hollister, C.D., 1972. Lithology of sediments from the western north Atlantic Leg 11 Deep Sea Drilling Project. In: Hollister, C.D., Ewing, J.I., et al. (Eds.), Init. Repts. DSDP. Washington (U.S. Govt. Printing Office), 11, 901-949.

Larson, P.B., Maher, K., Ramos, F.C., Chang, Z., Gaspar, M., Meinert, L.D., 2003. Copper isotope ratios in magmatic and hydrothermal ore-forming environments. Chem. Geol. 201, 337-350.

LeHuray, A.P., 1989. Native copper in ODP Site 642 tholeiites. In: Eldholm, O., Thiede, J., Taylor, E., et al. (Eds.), Proc. ODP, Sci. Results. College Station, TX (Ocean Drilling Program), 104, 411-417.

Leinen, M., Rea, D.K., Becker, K., Boulègue, J.J., Erzinger, J., Gieskes, J.M., Hobart, M.A., Kastner, M., Knüttel, S., Lyle, M.W., Moos, D., Newmark, R.L., Nishitani, T., Owen, R.M., Pearce, J.A., Romine, K., 1986. Site

597. In: Leinen, M., Rea, D.K., et al. (Eds.), Init. Repts. DSDP. Washington (U.S. Govt. Printing Office), 92, 25-96.

Maher, K.C., Larson, P.B., 2007. Variation in copper isotope ratios and controls on fractionation in hypogene skarn mineralization at Coroccohuayco and Tintaya, Peru. Econ. Geol. 102, 225-237.

Marchig, V., Erzinger, J., Heinze, P.M., 1986. Sediment in the black smoker area of the East Pacific Rise (18.5°S). Earth Planet. Sci. Lett. 79, 93-106.

Maréchal, C.N., Télouk, P., Albarède, F., 1999. Precise analysis of copper and zinc isotopic compositions by plasma-source mass spectrometry. Chem. Geol. 156, 251-273.

Markl, G., Lahaye, Y., Schwinn, G., 2006. Copper isotopes as monitors of redox processes in hydrothermal mineralization. Geochim. Cosmochim. Acta 70, 4215-4228.

Mason, T.F.D., Weiss, D.J., Chapman, J.B., Wilkinson, J.J., Tessalina, S.G., Spiro, B., Horswood, M.S.A., Spratt, J., Coles, B.J., 2005. Zn and Cu isotopic variability in the Alexandrinka volcanic-hosted massive sulphide (VHMS) ore deposit, Urals, Russia. Chem. Geol. 221, 170-187.

Mathur, R., Ruiz, J., Titley, S., Liermann, L., Buss, H., Brantley, S., 2005. Cu isotopic fractionation in the supergene environment with and without bacteria. Geochim. Cosmochim. Acta 69, 5233-5246.

Mathur, R., Titley, S., Barra, F., Brantley, S., Wilson, M., Phillips, A., Munizaga, F., Makseav, V., Vervoort, J., Hart, G., 2009. Exploration potential of Cu isotope fractionation in Porphyry Copper deposits. J. Geochem. Explor. 102, 1-6.

Miller, C., Thöni, M., Frank, W., Schuster, R., Melcher, F., Meisel, T., Zanetti, A., 2003. Geochemistry and tectonomagmatic affinity of the Yungbwa ophiolite, SW Tibet. Lithos 66, 155-172.

Minniti, M., Bonavia, F.F., 1984. Copper-ore grade hydrothermal mineralization discovered in a seamount in the Tyrrhenian Sea (Mediterranean): Is mineralization related to porphyry-copper or to base metal lodes? Mar. Geol. 59, 271-282.

Moeller, K., Schoenberg, R., Pedersen, R.-B., Weiss, D., Dong, S., 2012. Calibration of the new certified reference materials ERM-AE633 and ERM-AE647 for copper and IRMM-3702 for zinc isotope amount ratio determinations. Geostand. Geoanal. Res. 36, 177-199.

Mottl, M.J., McConachy, T.F., 1990. Chemical processes in buoyant hydrothermal plumes on the East Pacific Rise near 21°N. Geochim. Cosmochim. Acta 54, 1911-1927.

Moynier, F., Koeberl, C., Beck, P., Jourdan, F., Telouk, P., 2010. Isotopic fractionation of Cu in tektites. Geochim. Cosmochim. Acta 74, 799-807.

Nagle, F., Fink, L.K., Boström, K., Stipp, J.J., 1973. Copper in pillow basalts from La Desirade, Lesser Antilles island arc. Earth Planet. Sci. Lett. 19, 193-197.

Nishitani, T., 1986. Electron microprobe and thermomagnetic analysis of basalt samples from Hole 597C. In: Leinen, M., Rea, D.K., et al. (Eds.), Init. Repts. DSDP. Washington (U.S. Govt. Printing Office), 92, 481-489.

Ono, S., Keller, N.S., Rouxel, O., Alt, J.C., 2012. Sulfur-33 constraints on the origin of secondary pyrite in altered oceanic basement. Geochim. Cosmochim. Acta 87, 323-834.

Ovenshine, A.T., Winkler, G.R., Andrews, P.B., Gostin, V.A., 1975. Chemical analyses and minor element composition of Leg 29 basalts. In: Kennett, J.P., Houtz, R.E., et al. (Eds.), Init. Repts. DSDP. Washington (U.S. Govt. Printing Office), 29, 1097-1102.

Palacios, C., Rouxel, O., Reich, M., Cameron, E.M., Leybourne, M.I., 2011. Pleistocene recycling of copper at a porphyry system, Atacama Desert, Chile: Cu isotope evidence. Miner. Deposita 46, 1-7.

Pearce, C.I., Pattrick, R.A.D., Vaughan, D.J., Henderson, C.M.B., van der Laan, G., 2006. Copper oxidation state in chalcopyrite: Mixed Cu d^9 and d^{10} characteristics. Geochim. Cosmochim. Acta 70, 4635-4642.

Peterson, C., Duncan, R., Scheidegger, K.F., 1986. Sequence and longevity of basalt alteration at Deep Sea Drilling Project Site 597. In: Leinen, M., Rea, D.K., et al. (Eds.), Init. Repts. DSDP. Washington (U.S. Govt. Printing Office), 92, 505-515.

Pinto, V.M., Hartmann, L.A., Wildner, W., 2011. Epigenetic hydrothermal origin of native copper and supergene enrichment in the Vista Alegre district, Paraná basaltic province, southernmost Brazil. International Geology Review 53, 1163-1179.

Pokrovsky, O.S., Viers, J., Emnova, E.E., Kompantseva, E.I., Freydier, R., 2008. Copper isotope fractionation during its interaction with soil and aquatic microorganisms and metal oxy(hydr)oxides: Possible structural control. Geochim. Cosmochim. Acta 72, 1742-1757.

Puchelt, H., Prichard, H.M., Berner, Z., Maynard, J., 1996. Sulfide mineralogy, sulfur content and sulfur isotope composition of mafic and ultramafic rocks from Leg 147. In: Mével, C., Gillis, K.M., Allan, J.F., Meyer, P.S., (Eds.), Proc. ODP, Sci. Results. 147, 91-101.

Ramdohr, P., 1980. The Ore Minerals and Their Intergrowths. Pergamon Press, Oxford.

Roberts, D.G., Schnitker, D., Backman, J., Baldauf, J.G., Desprairies, A., Homrighausen, R., Huddlestun, P., Kaltenback, A.J., Keene, J.B., Krumsiek, K.A.O., Morton, A.C., Murray, J.W., Westberg-Smith, J., Zimmerman, H.B., 1984. Sites 552-553. In: Roberts, D.G., Schnitker, D., et al. (Eds.), Init. Repts. DSDP. Washington (U.S. Govt. Printing Office), 81, 31-233.

Rouxel, O., Dobbek, N., Ludden, J., Fouquet, Y., 2003. Iron isotope fractionation during oceanic crust alteration. Chem. Geol. 202, 155-182.

Rouxel, O., Fouquet, Y., Ludden, J.N., 2004. Copper isotope systematics of the Lucky Strike, Rainbow, and Logatchev sea-floor hydrothermal fields on the Mid-Atlantic Ridge. Econ. Geol. 99, 585-600.

Rouxel, O., Ono, S., Alt, J., Rumble, D., Ludden, J., 2008. Sulfur isotope evidence for microbial sulfate reduction in altered oceanic basalts at ODP Site 801. Earth Planet. Sci. Lett. 268, 110-123.

Schlanger, S.O., Jackson, E.D., Boyoce, R.E., Cook, H.E., Jenkyns, H.C., Johnson, D.A., Kaneps, A.G., Kelts, K.R., Martini, E., McNulty, C.L., Winterer, E.L., 1976. Site 317. In: Schlanger, S.O., Jackson, E.D., et al. (Eds.), Init. Repts. DSDP. Washington (U.S. Govt. Printing Office), 33, 161-300.

Seo, J.H., Lee, S.K., Lee, I., 2007. Quantum chemical calculations of equilibrium copper (I) isotope fractionations in ore-forming fluids. Chem. Geol. 243, 225-237.

Seyfried, Jr. W.E., Bischoff, J.L., 1979. Low temperature basalt alteration by seawater: an experimental study at 70°C and 150°C. Geochim. Cosmochim. Acta 43, 1937-1947.

Sharkov, E.V., Abramov, S.S., Simonov, V.A., Krinov, D.I., Skolotnev, S.G., Bel'tenev, V.E., Bortnikov, N.S., 2007. Hydrothermal alteration and sulfide mineralization in gabbroids of the Markov Deep (Mid-Atlantic Ridge, 6°N). Geology of Ore Deposits 49, 467-486.

Shields, W.R., Goldich, S.S., Garner, E.L., Murphy, T.J., 1965. Natural variations in the abundance ratio and the atomic weight of copper. J. Geophys. Res. 70, 479-491.

Siesser, W.G., 1978. Native copper in DSDP Leg 40 sediments. In: Bolli, H.M., Ryan, W.B.F., et al. (Eds.), Init. Repts. DSDP. Washington (U.S. Govt. Printing Office), Supplement to volumes 38, 39, 40 and 41, 761-765.

Singer, P.C., Stumm, W., 1970. Acidic mine drainage: The rate-determining step. Science 167, 1121-1123.

Takano, S., Tanimizu, M., Hirata, T., Sohrin, Y., 2013. Determination of isotopic composition of dissolved copper in seawater by multi-collector inductively coupled plasma mass spectrometry after pre-concentration using an ethylenediaminetriacetic acid chelating resin. Anal. Chim. Acta 784, 33-41.

Talwani, M., Udintsev, G.B., Bjørklund, K., Caston, V.N.D., Faas, R.W., van Hinte, J.E., Kharin, G.N., Morris, D.A., Müller, C., Nilsen, T.H., Warnke, D.A., White, S.M., 1976. Sites 338-343. In: Talwani, M., Udintsev, G.B., et al. (Eds.), Init. Repts. DSDP. Washington (U.S. Govt. Printing Office), 38, 151-387.

Teagle, D.A.H., Alt, J.C., 2004. Hydrothermal alteration of basalts beneath the Bent Hill massive sulfide deposit, Middle Valley, Juan de Fuca Ridge. Econ. Geol. 99, 561-584.

Thompson, C.M., Ellwood, M.J., Wille, M., 2013. A solvent extraction technique for the isotopic measurement of dissolved copper in seawater. Anal. Chim. Acta 775, 106-113.

Thompson, G., Bryan, W.B., Frey, F.A., Sung, C.M., 1974. Petrology and geochemistry of basalts and related rocks from Sites 214, 215, 216, DSDP Leg 22, Indian Ocean. In: von der Borch, C.C., Sclater, J.G., et al. (Eds.), Init. Repts. DSDP. Washington (U.S. Govt. Printing Office), 22, 213-265.

Tossell, J.A., 2005. Calculating the partitioning of the isotopes of Mo between oxidic and sulfidic species in aqueous solution. Geochim. Cosmochim. Acta 69, 2981-2993.

Vance, D., Archer, C., Bermin, J., Perkins, J., Statham, P., Lohan, M., Ellwood, M., Mills, R., 2008. The copper isotope geochemistry of rivers and the oceans. Earth Planet. Sci. Lett. 274, 204-213.

von der Borch, C.C., Sclater, J.G., Gartner, S., Hekinian, R., Johnson, D.A., McGowran, B., Pimm, A.C., Thompson, R.W., Veevers, J.J., Waterman, L.S., 1974. Site 216. In: von der Borch, C.C., Sclater, J.G., et al. (Eds.), Init. Repts. DSDP. Washington (U.S. Govt. Printing Office), 22, 213-265.

Walker, E.C., Cuttitta, F., Senftle, F.E., 1958. Some natural variations in the relative abundance of copper isotopes. Geochim. Cosmochim. Acta 15, 183-194.

Wang, C.Y., Zhou, M.-F., Qi, L., Hou, S.G., Gao, H.G., Zhang, Z.W., Malpas, J., 2006. The Zhaotong native copper deposit associated with the Permian Emeishan flood basalts, Yunnan, Southwest China. International Geology Review 48, 742-753.

Wheat, C.G., Mottl, M.J., 2000. Composition of pore and spring waters from Baby Bare: Global implications of geochemical fluxes from a ridge flank hydrothermal system. Geochim. Cosmochim. Acta 64, 629-642.

Wheat, C.G., Elderfield, H., Mottl, M.J., Monnin, C., 2000. Chemical composition of basement fluids within an oceanic ridge flank: Implications for along-strike and across-strike hydrothermal circulation. J. Geophys. Res. 105, B6, 13,437-13,447.

Wheat, C.G., Mottl, M.J., Rudnicky, M., 2002. Trace element and REE composition of a low-temperature ridge-flank hydrothermal spring. Geochim. Cosmochim. Acta 66, 3693-3705.

Wheat, C.G., Jannasch, H.W., Kastner, M., Plant, J.N., DeCarlo, E.H., 2003. Seawater transport and reaction in upper oceanic basaltic basement: chemical data from continuous monitoring of sealed boreholes in a ridge flank environment. Earth Planet. Sci. Lett. 216, 549-564.

Wheat, C.G., Jannasch, H.W., Fisher, A.T., Becker, K., Sharkey, J., Hulme, S., 2010. Subseafloor seawater-basalt-microbe reactions: Continuous sampling of borehole fluids in a ridge flank environment. Geochem. Geophys. Geosyst. 11, Q07011, doi:10.1029/2010GC003057.

Zemmels, I., Cook, H.E., Hathaway, J.C., 1972. X-ray mineralogy studies - Leg 11. In: Hollister, C.D., Ewing, J.I., et al. (Eds.), Init. Repts. DSDP. Washington (U.S. Govt. Printing Office), 11, 729-789.

Zhu, X.K., O'Nions, R.K., Guo, Y., Belshaw, N.S., Rickard, D., 2000. Determination of natural Cu-isotope variation by plasma-source mass-spectrometry: implications for use as geochemical tracers. Chem. Geol. 163, 139-149.

Zhu, X.K., Guo, Y., Williams, R.J.P., O'Nions, R.K., Matthews, A., Belshaw, N.S., Canters, G.W., de Waal, E.C., Weser, U., Burgess, B.K., Salvato, B., 2002. Mass fractionation processes of transition metal isotopes. Earth Planet. Sci. Lett. 200, 47-62.

Figure captions

Fig. 1. Map with locations and lithologic columns for DSDP/ODP sites with native Cu occurrences discussed in this paper. 1 = spreading centers; 2 = subduction zones; 3 = number and position of DSDP/ODP sites with native Cu occurrences analyzed in this study; 4 = number and position of DSDP/ODP sites with reported native Cu occurrences not found and analyzed in this study; 5 = number and position of DSDP/ODP sites with reported native Cu occurrences not provided for this study; 6 = silty clay; 7 = hemipelagic clay; 8 = nannofossil ooze; 9 = dolomite; 10 = radiolarian ooze; 11 = pelagic clay; 12 = scattered glauconite grains; 13 = volcanic ash; 14 = sapropels; 15 = nanno chalk; 16 = limestone; 17 = igneous rocks (basalts ± andesites); 18 = dikes; 19 = native Cu occurrences investigated in this work.

Fig. 2. (A) Photograph (stereo-microscope) of a leaf of native Cu (dark red) with specks of light blue mineral phase from an open crack in basalt [sample 22-216-37-4 (114-117)]; (B) micrograph (reflected light, optical microscope) of native Cu particle in basalt rock [sample 92-597C-4-2 5E (134-135), polished section]; (C) micrograph (reflected light, optical microscope) of native Cu vein in basalt rock [sample 92-597C-7-3 16 (135-138), polished section]; (D) SEM micrograph (SEI) of native Cu crystals [sample 11-105-38-2 (110-112)]; (E) SEM micrograph (SEI) of the surface of a native Cu leaf [sample 22-216-37-4 (114-117)]; (F) SEM micrograph (SEI) of light blue mineral phase (Cu, O, Cl composition; EDS studies) on the surface of a native Cu particle [sample 22-216-37-4 (114-117)]; (G) SEM micrograph (SEI) of light blue mineral phase (Cu, S, Cl, O composition; EDS studies) on the surface of a native Cu particle [sample 92-597C-7-3 16 (135-138)]; (H) SEM micrograph (SEI) of light blue mineral phase (Cu, Cl, O composition; EDS studies) on the surface of a native Cu particle [sample 22-216-37-4 (114-117)].

Fig. 3. Reflectance spectra of native Cu [22-216-37-4 (114-117)] obtained in air (closed circles) and in oil (closed squares) compared with spectra of native Cu (QDF3) from the Botallack mine, Cornwall, UK (Criddle and Stanley, 1993) measured in air (open circles) and oil (open squares).

Fig. 4. RBS depth profiles of the main elements detected through PIXE point analyses at natural surface of native Cu grains: (A) sample 22-216-37-4 (114-117); (B) sample 92-597C-4-2D (60-65). Analyses #1 and #2 as in Table 2.

Fig. 5. Eh–pH phase diagrams for the Cu system calculated at P = 1 atm, T = 60°C, a[Cu] = 5.6E-9, and a[Cl] = 0.55. (a) stability fields of Cu fluid speciation and minerals with a[SO_4] = 0.018 added to the system; (b) stability fields of Cu fluid speciation and minerals with a[SO_4] = 0.018 and a[Fe] = 1E-9 added to the system; (c) stability fields of the S fluid speciation under the same system conditions as plot (a); (d) stability fields of Cu fluid speciation and minerals with no SO_4 and Fe, where native Cu is most likely to form; (e) stability fields of Cu fluid speciation and minerals in a system with no SO_4, but with a[Fe] = 1E-9 added to the system.

Fig. 6. Different Cu-isotope pools at the seafloor and model diagram of Cu^0 precipitation in the oceanic basement as a result of low-temperature hydrothermal activity. Conception for low-temperature ("cool" and "warm") hydrothermal systems is after Wheat et al. (2002). Cold and oxic seawater enters basement at the MOR crest, alters (warms and becomes anoxic) during its flow within the crust and vents out the discharge zones. Favorable conditions for Cu^0 precipitation (Fig. 5d) are attained in the anoxic and H_2S-deficient domains achieved due to the very limited SO_4^{2-} reduction extent in the volcanic basement (Ono et al., 2011), or diffusing exchange of SO_4^{2-} (i.e., net loss) with the overlying organic-rich sediment (Elderfield et al., 1999). In addition to the low background Cu flux with lithogenic matter the sediment blanket obtains hydrogenous (adsorbed from seawater on hydrogenous Mn-Fe-oxyhydroxides) and hydrothermal (hydrothermal plume fallout) Cu that might eventually be diagenetically remobilized and reprecipitated as Cu^0.

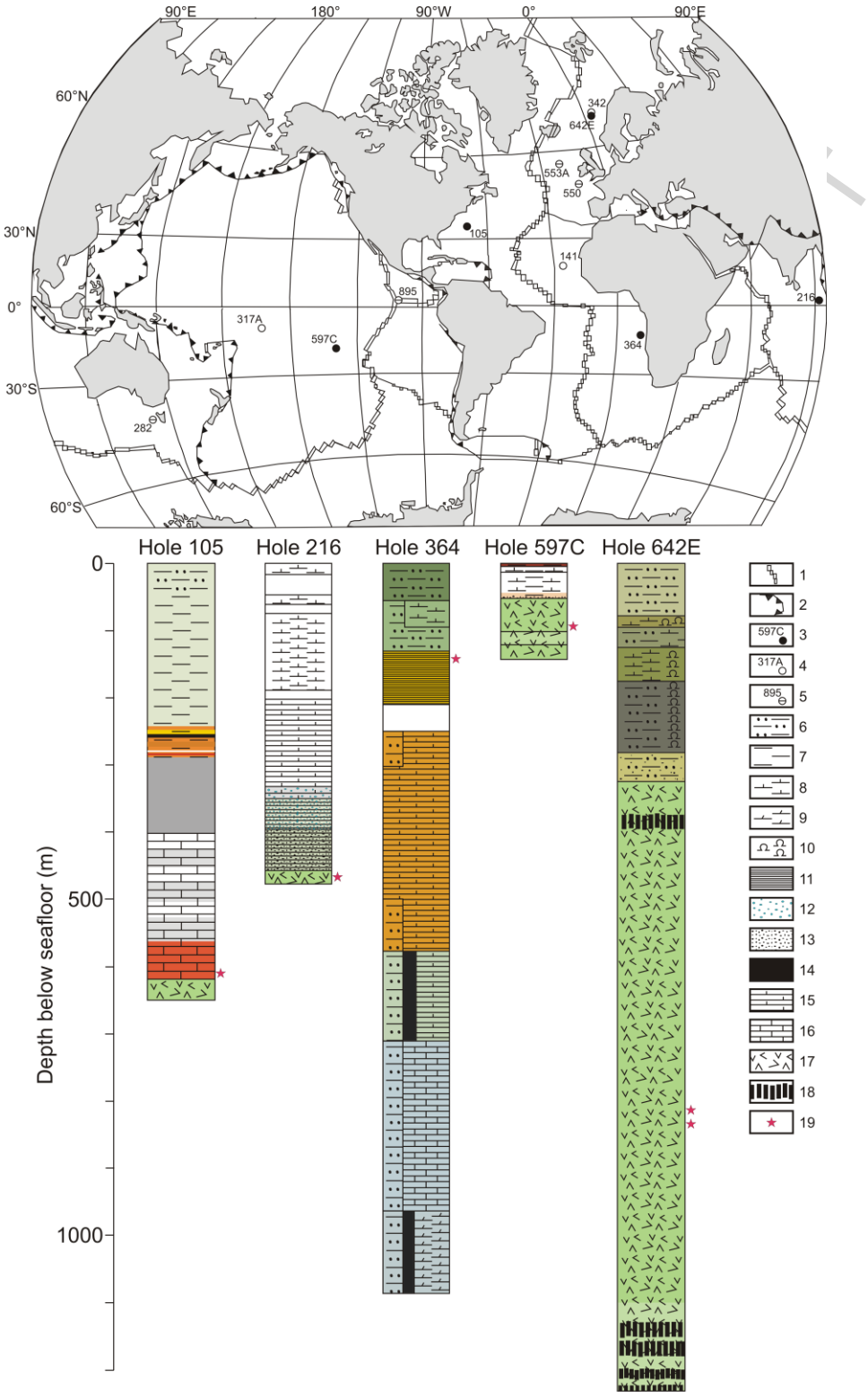

Fig. 1

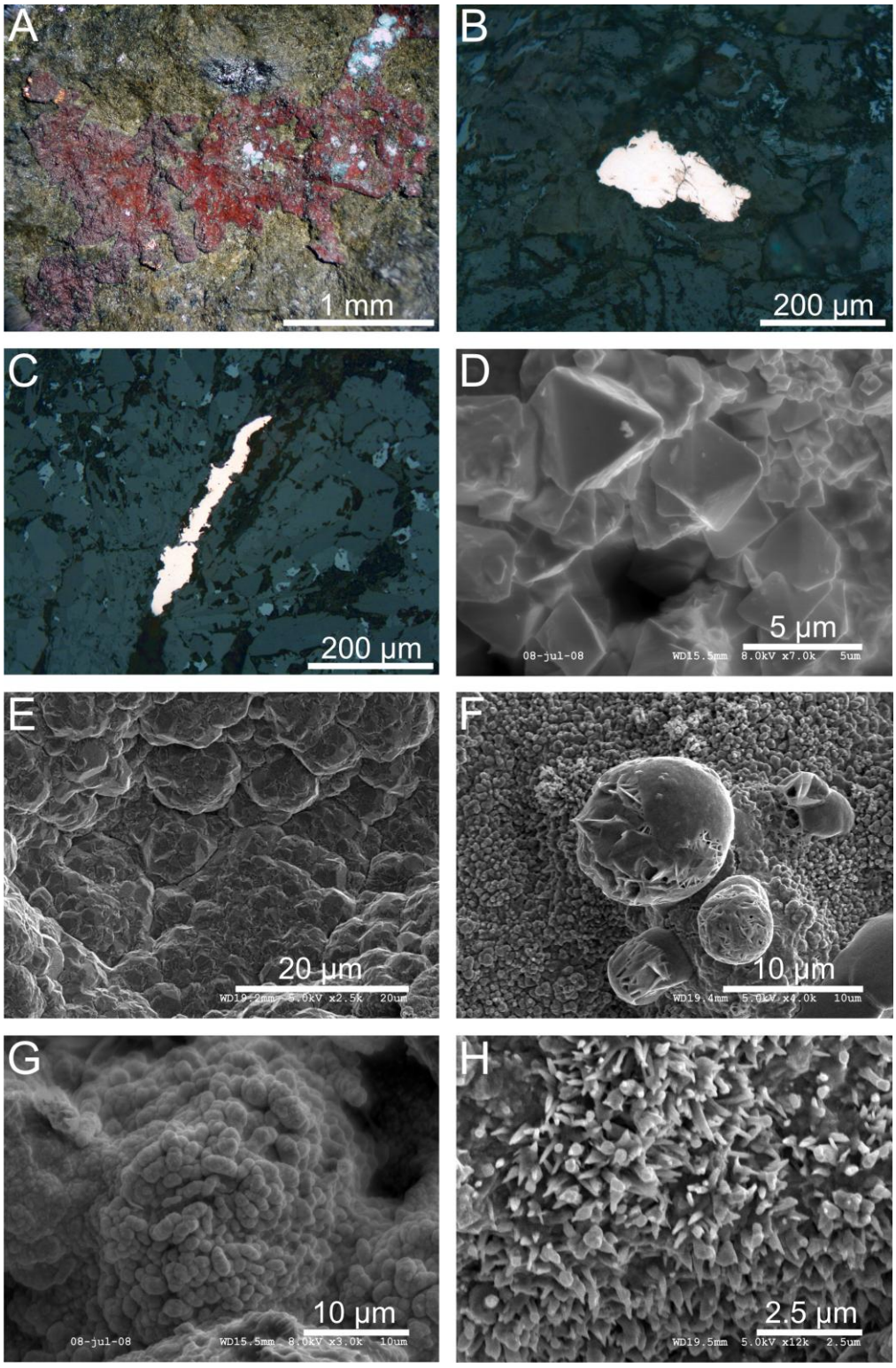

Fig. 2

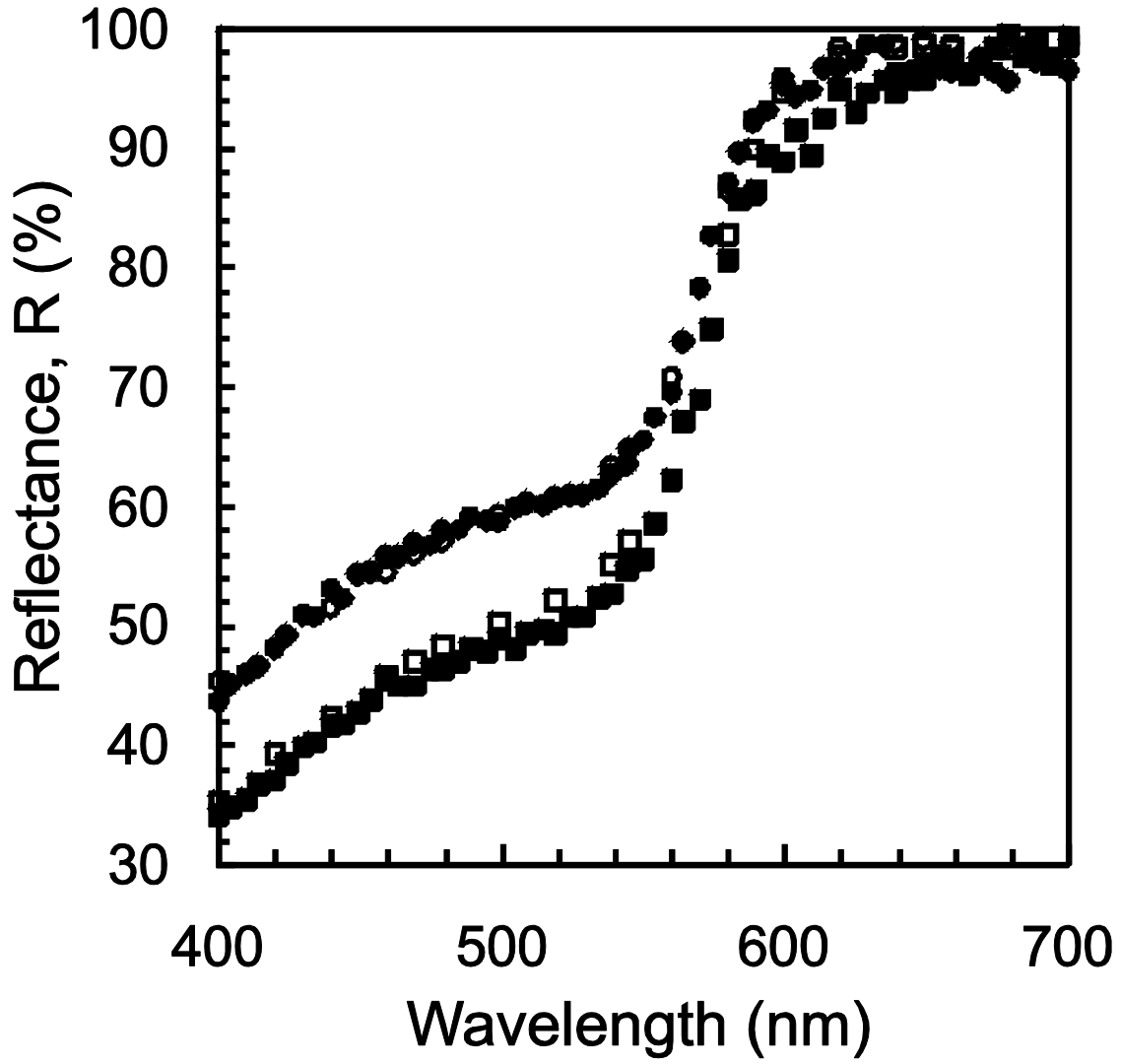

Fig. 3

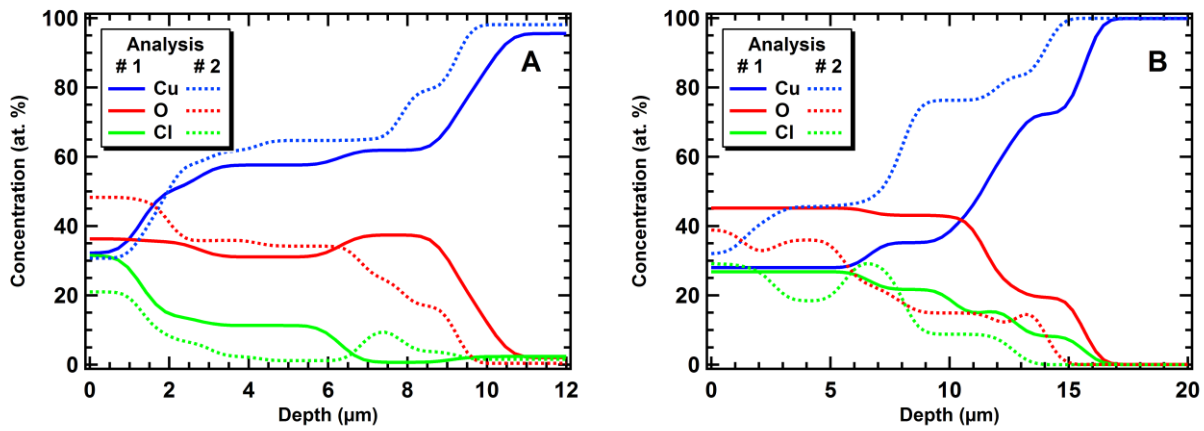

Fig. 4

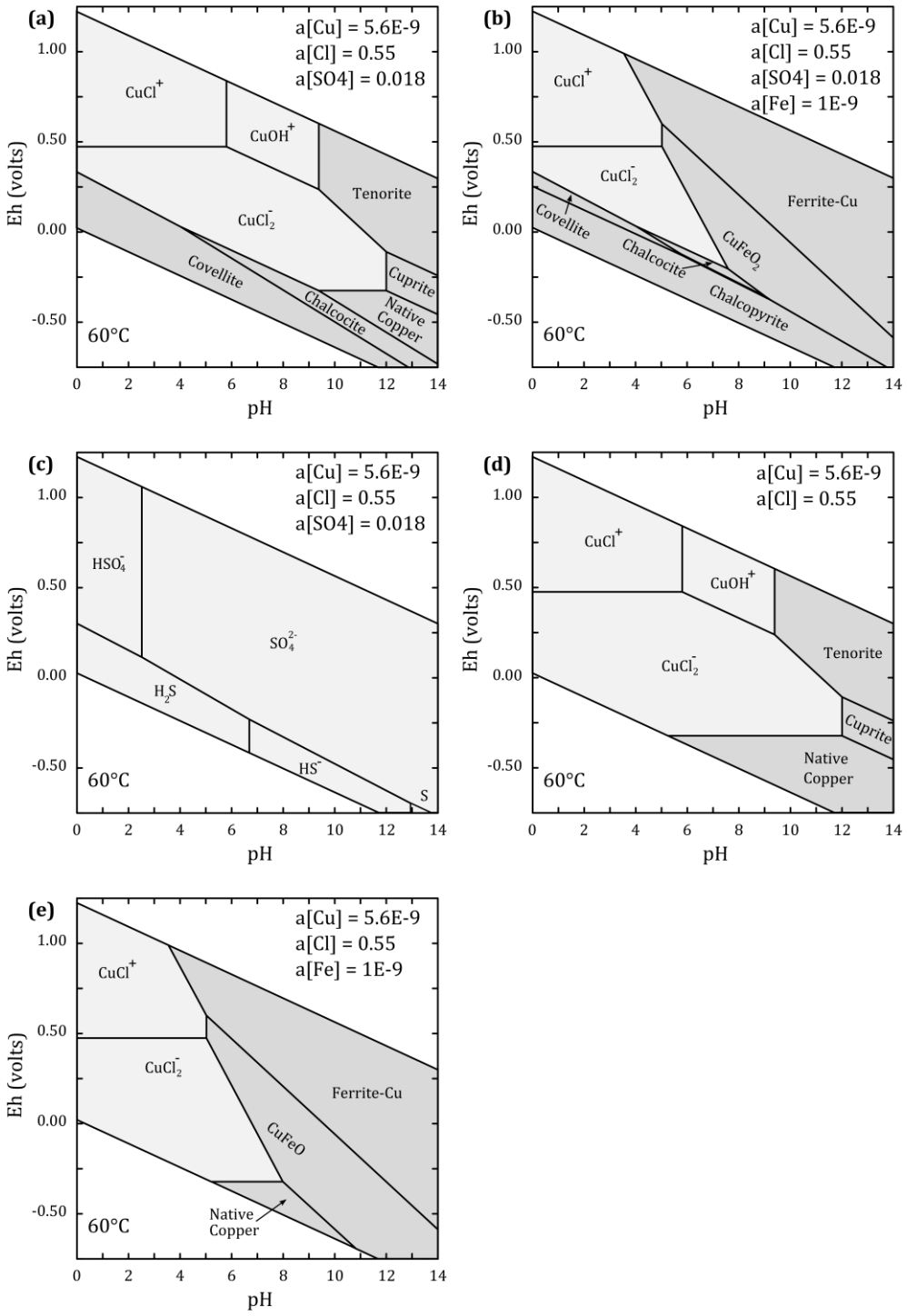

Fig. 5

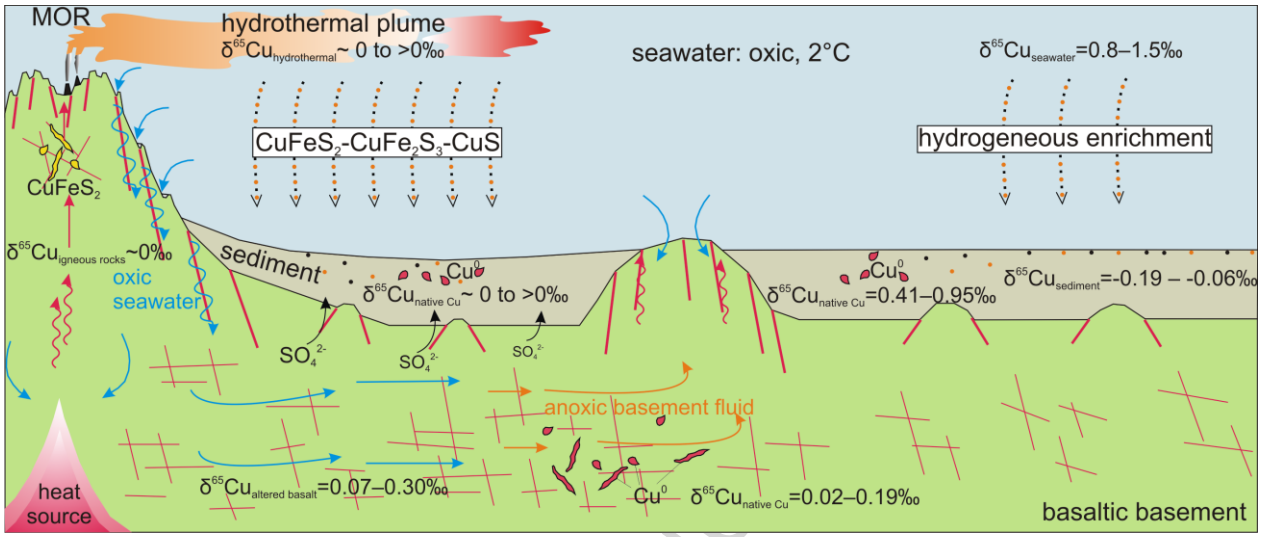

Fig. 6

Table 1
Sample locations for investigated native Cu occurrences.

Location	Sample ID Leg-Hole-Core-Section (Horizon)	Latitude	Longitude	Depth (m)	Original description in DSDP/ODP reports
Lower continental rise hills, North Atlantic Ocean	*11-105-38-2 (110-112)*[1]	34°53.72'N	69°10.40'W	5245	native Cu veinlet in clayey reddish-brown limestone
North of Cape Verde Islands, North Atlantic Ocean	14-141-6-5 (140-142)	19°25.16'N	23°59.91'W	4148	irregular network of red strands in nanno chalk
Crest of Ninetyeast Ridge, Equatorial Indian Ocean	*22-216-37-4 (114-117)*	1°27.73'N	90°12.48'E	2262	leafs of native Cu in fine-grained basalt
Manihiki Plateau, Central South Pacific Ocean	33-317A-22-2 (120-123)	11°00.09'S	162°15.78'W	2598	native Cu flakes in red volcanogenic sandstone
	33-317A-23-3 (9-11)				native Cu flakes in volcanogenic sandstone
	33-317A-23-4 (140-144)				native Cu flakes in volcanogenic sandstone
	33-317A-25-5 (40-42)				grains of native Cu in volcanogenic sandstone
Norwegian Sea	38-342-8-2 (32-34)	67°57.04'N	04°56.02'E	1303	small vesicles with native Cu in phyric basalt
	38-342-8-2 (120-122)				small vesicles with native Cu in phyric basalt
	38-342-8-3 (95-97)				small vesicles with native Cu in phyric basalt
	38-342-8-4 (136-141)				small vesicles with native Cu in phyric basalt
Angola continental margin, South Atlantic Ocean	*40-364-5-2 (19-21)*	11°34.32'S	11°58.30'E	2448	native Cu flakes in yellowish brown pelagic clay
Western flank of the East Pacific Rise	*92-597C-4-1C (33-35)*	18°48.43'S	129°46.22'W	4164	Cu vein in aphyric basalt
	92-597C-4-1E (80-82)				Cu vein in aphyric basalt
	92-597C-4-2D (60-65)				Cu vein in aphyric basalt
	92-597C-4-2 5E (134-135)				Cu vein in aphyric basalt
	92-597C-4-4 2E				Cu vein in aphyric basalt

	(104-107)				
	92-597C-4-4 2F (120-124)				Cu vein in aphyric basalt
	92-597C-7-3 15 (121-125)				Cu vein in fine-grained aphyric basalt
	92-597C-7-3 16 (135-138)				Cu vein in fine-grained aphyric basalt
Vøring Plateau, Norwegian Sea	*104-642E-64R-2 (78-80)*	67°13.5'N	2°55.7'E	1286	Cu vein in fine-grained, aphyric, gray basalt
	104-642E-66R-2 (19-22)				Cu vein in fine-grained, phyric, gray basalt
	104-642E-69R-2 (112-115)				Cu blebs in dark, red brown tuff
	104-642E-85R-5 (86-88)				Cu blebs in dark, red brown, well sorted, vitric, lithic tuff

[1] In italic, samples where native Cu has been found and analyzed in the course of this study.

Table 2

Composition (PIXE analyses on natural surface)[1] of native Cu occurrences.

Sample ID Leg-Hole-Core-Section (Horizon)	Analysis #	Cu wt. %	O[2]	Cl	Fe	Si	Ca	As ppm	K	Mn
22-216-37-4 (114-117)	1	80.7	10.3	8.93	0.10	b.d.l.[3]	b.d.l.	b.d.l.	b.d.l.	b.d.l.
	2	87.7	11.2	0.79	0.29	b.d.l.	b.d.l.	b.d.l.	b.d.l.	b.d.l.
92-597C-4-2D (60-65)	1	73.4	9.59	16.3	0.44	b.d.l.	0.18	856	b.d.l.	b.d.l.
	2	74.5	11.7	10.0	2.28	1.25	0.17	522	395	222

[1] Average concentrations for point measurements under the assumption that the Cu^0 particles are homogeneous in depth and the main additional elements in the surface films are O and Cl (see the RBS data). It should be noted that the samples are inhomogeneous and therefore these results contain systematic deviations.

[2] Calculated from concentrations of the other elements assuming they are present in their oxidized form and using their stoichiometric relations with O. The assumption of oxidized states is justified by the simultaneous RBS measurements that show presence of O in the outer ~10 µm-film of the samples.

[3] b.d.l. = below detection limit.

Table 3
Cu-isotope composition of native Cu occurrences, their host rocks and some reference materials.

Sample ID Leg-Hole-Core-Section (Horizon)	Type	Cu ppm	N[1]	δ^{65}Cu ‰	1SD
11-105-38-2 (110-112)	native Cu		6	0.41	0.03
	native Cu		4	0.49	0.07
	bluish phase around Cu^0		6	0.21	0.03
	bluish phase around Cu^0		4	-0.09	0.04
	clayey reddish-brown limestone	75	4	-0.06	0.01
22-216-37-4 (114-117)	native Cu		6	0.18	0.02
	native Cu		4	0.14	0.03
	native Cu		4	0.16	0.03
	native Cu		4	0.19	0.02
	basalt	>2000	4	0.30	0.02
40-364-5-2 (19-21)	native Cu with bluish phase around		4	0.95	0.06
	yellowish brown pelagic clay	35	4	-0.19	0.02
92-597C-7-3 16 (135-138)	native Cu		6	0.02	0.01
	basalt	325	4	0.07	0.03
1149A-20X1, 140[2]	deep-sea clays	192	4	0.01	0.02
1149C-02W1, 31[2]	Mn-rich cherts	504	4	0.37	0.03
1149C-11R1, 19/D[2]	altered basalt	63	4	0.00	0.03
801C-44R3, 32/V+H[2]	altered basalt	148	4	0.11	0.04

[1] Number of duplicates analysed.
[2] Samples described in Rouxel et al. (2003).

Table 4

Cu-isotope composition of native Cu occurrences from different deposits.

Sample ID	Mineral	Locality	Deposit type	δ^{65}Cu ‰	1SD	Reference
84	native Cu	Pima, Arizona, USA	pyrometasomatic	2.0		Shields et al., 1965
85	- " -	Soudan mine, Minnesota, USA		0.9		- " -
86	- " -	Azaruzawa, Rikuchiu, Japan		-0.3		- " -
87	- " -	Copper River, Alaska, USA	hydrothermal	-0.3		- " -
88	- " -	Lake Superior district, Michigan, USA	- " -	-1.0		- " -
89	- " -	Corocoro, Bolivia	- " -	-1.1		- " -
90	- " -	Painesdale, Michigan, USA	- " -	-1.3		- " -
LS-7	- " -	Trimountain Mine, Michigan, USA	- " -	0.27		Larson et al., 2003
LS-10	- " -	Baltic Mine, Michigan, USA	- " -	0.29 (mean)	0.04	- " -
LS-12	- " -	Centennial Mine, Michigan, USA	- " -	0.26		- " -
LS-45	- " -	Isle Royale Mine, Michigan, USA	- " -	0.34		- " -
LS-48	- " -	Wolverine Mine, Michigan, USA	- " -	0.30		- " -
LS-51	- " -	Copper Falls Mine, Michigan, USA	- " -	0.02 (mean)	0.01	- " -
Ray-1	- " -	Ray Mine, Arizona, USA	supergene	-0.04 (mean)	0.04	- " -
Ray-2	native Cu + cuprite	- " -	- " -	1.26		- " -
Ray-2b	native Cu	- " -	- " -	0.72		- " -
CCP-2	- " -	Ccatun Pucara, Tintaya, Peru	- " -	-0.83		- " -
	- " -	Ray Mine, Arizona, USA	- " -	-3.03	0.04	Maréchal et al., 1999
OUM22647	- " -	Bisbee, Arizona, USA		-0.2		Zhu et al., 2000
OUM15126	- " -	Michigan, USA	hydrothermal	0.45		- " -
OUM15120	- " -	Lake Superior, North America	- " -	0.54		- " -
OUM00061	- " -	Yekaterinburg, Russia		-0.33		- " -
OUM15127	- " -	Cornwall, England		0.41		- " -
OUM00078	- " -	St. Cleer, Cornwall, England		1.25		- " -
NNB82	- " -	Neubulach near Calw, Germany	supergene	-0.46	0.02	Markl et al., 2006
Cu3	- " -	Prosper near Rippoldsau, Germany	- " -	0.39	- " -	- " -
Arizona Cu	- " -	Morenci, Arizona, USA		-0.51	0.07	Ikehata et al., 2008
Mio 7-4	- " -	Mio mine, Sanbagawa metamorphic belt, Japan	supergene	1.57	0.02	Ikehata et al., 2011
Mio 7-5	- " -	- " -	- " -	1.71	0.03	- " -
Mio 7-6	- " -	- " -	- " -	1.65	0.02	- " -
Mio 7-7	- " -	- " -	- " -	1.62	0.03	- " -
Mio 8-4	- " -	- " -	- " -	1.45	0.03	- " -
Mio 8-5	- " -	- " -	- " -	1.54	0.02	- " -
Mio 8-6	- " -	- " -	- " -	1.43	0.02	- " -
Mio 8-7	- " -	- " -	- " -	1.56	0.03	- " -